Available online at www.CivileJournal.org

Civil Engineering Journal

(E-ISSN: 2476-3055; ISSN: 2676-6957)

Vol. 8, No. 12, December, 2022

Optimization of Green Concrete Containing Fly Ash and Rice Husk Ash Based on Hydro-Mechanical Properties and Life Cycle Assessment Considerations

Kennedy C. Onyelowe [1], Ahmed M. Ebid [2*], Hisham A. Mahdi [2], Atefeh Soleymani [3], Hashem Jahangir [4], Farshad Dabbaghi [5]

[1] *Department of Civil Engineering, Michael Okpara University of Agriculture Umudike, 440109, Umuahia, Nigeria.*

[2] *Faculty of Engineering and Technology, Future University in Egypt, New Cairo 11865, Egypt.*

[3] *Department of Civil Engineering, Shahid Bahonar University of Kerman, Kerman, Iran.*

[4] *Department of Civil Engineering, University of Birjand, Birjand, Iran.*

[5] *Department of Civil Engineering, Babol Norshivani University of Technology, Mazandaran, Iran.*

Received 24 July 2022; Revised 07 November 2022; Accepted 14 November 2022; Published 01 December 2022

Abstract

The development of sustainable concrete in achieving the developmental goals of the United Nations in terms of sustainable infrastructure and innovative technology forms part of the focus of this research paper. In order to move towards sustainability, the utilization of the by-products of agro-industrial operations, which are fly ash (FA) and rice husk ash (RHA), in the production of concrete has been studied. Considering the environmental impact of concrete constituents, multiple mechanical and hydraulic properties of fly ash (FA) and rice husk ash (RHA) concrete have been proposed using intelligent techniques; artificial neural network (ANN) and evolutionary polynomial regressions (EPR). Also, an intelligent mix design tool/chart for this case under study is proposed. Multiple data points of concrete materials, which were further reduced to ratios as follows; cement to binder ratio (C/B), aggregate to binder ratio (Ag/B), and plasticizer to binder ratio (PL/B) were used in this exercise. At the end of the protocol, it is observed that the constituents' ratios are dependent on the behavior of the whole, which can be solved by using the proposed model equations and mix design charts. The models performed optimally, as none showed any performance below 80%. However, ANN, which predicted Fc03, Fc07, Fc28, Fc60, Fc90, Ft28, Ff28 & Fb28, S, Ec28 & K28, and P with an accuracy of greater than 95% each with average error of less than 9.4% each, is considered the decisive technique in predicting all the studied concrete properties, including the life cycle assessment potential of the concrete materials.

Keywords: Fly Ash; Rice Husk Ash; Concrete Hydro-Mechanical Properties; Sustainable Concrete; Concrete Life Cycle Assessment.

1. Introduction

The worldwide construction sector has profited from the world's fast-growing economy during the twentieth century and continues to achieve new heights [1]. Sustainability in the building industry is among the most crucial needs of developing countries because of limited natural resources and growing carbon dioxide emissions from massive cement and concrete manufacturing. Due to the breakdown of utilized $CaCO_3$ in the cement clinker and the burning of fuel, cement production is responsible for emitting approximately 5 to 7% of carbon dioxide emissions worldwide [2–7]. As

* Corresponding author: ahmed.abdelkhaleq@fue.edu.eg

http://dx.doi.org/10.28991/CEJ-2022-08-12-018

a result, green concrete development is now a big problem [8]. Pursuant to the IEA (International Energy Agency), lowering the clinker to cement proportion from 65% to 60% by 2050 will diminish total carbon dioxide (CO_2) emissions related to cement manufacturing by up to 37 percent. The use of ordinary Portland cement (OPC) can be decreased if a percentage of the concrete production can be substituted with recycled concrete aggregates, cutting greenhouse gas emissions associated with cement manufacturing [9–11]. Palm oil shells (POS), sugarcane bagasse ash (SCBA), corncob, elephant grass ash (EGA), wood ash, coir coconut fiber, rice husk ash (RHA), tobacco product waste (TPW), and other agricultural by-products have all been shown to be useful as additions [10, 12–18]. Some by-products give advantages such as enhanced strength and durability, economic savings from surplus cement and natural aggregates, and ecological advantages like fewer carbon dioxide emissions and simpler disposal of harmful waste materials [1, 19–23].

To lessen the environmental effects, eco-friendly green concrete can be described as the substitution of a percentage of cement with natural or recyclable resources [24, 25]. Industrial wastes from power plants with substantial discharges are known as fly ash (FA). Its inadequate comprehensive usage results in a massive build-up that encroaches on arable land, produces dust, and pollutes water supplies. However, because of its high aluminum and silicon content, it has the potential for pozzolanic properties when activated by grinding, calcining, and other methods, and thus can be used as supplemental cementitious materials (SCMs). Mineral admixtures are effective SCMs that not only conserve cement but also alleviate numerous environmental issues created by industrial waste [25–27]. Furthermore, it assists businesses and governments in lowering the cost of pollution control. It is well accepted that using industrial waste as a mineral additive in green concrete casting offers several benefits and promising future prospects [28].

Rice husk is one of the most common agricultural wastes extracted from rice grain pods during milling [29, 30]. Rice husk ash (RHA), like FA, is a pozzolanic material with a very high level of reactivity that may be used in concrete mix designs to replace up to 30 percent of the total OPC. Concrete produced using RHA is still an ideal material in the United States. FA supply has dropped in recent years due to decreasing coal use, overall economic stagnation, and regulatory hurdles, despite a rise in its use in concrete industry. However, RHA has the ability to satisfy demand as FA supplies decline [30]. Concrete has been proven to benefit from the use of rice husk ash and other mineral admixtures. Due to its wide surface area, RHA is comparable to other pozzolans used in concrete production, notably micro silica [31–34]. The compressive strength of concrete was substantially improved and the permeability of the concrete was significantly lowered by adding RHA to the mix [30].

Amin et al. [35] researched the impact of optimal replacement levels of rice husk ash and FA on the fresh and hardened features of concrete mixes. Replacement levels from OPC amounts were 10, 20, and 30% for each recycled material, respectively (RHA and FA). Hardened concrete was tested mechanically for bond strength, modulus of Elasticity, modulus of rupture, splitting tensile strength, and compression strength. When compared to the control combination, test findings showed that the fly and rice husk ash improved physical and mechanical properties. The cementitious concentration of 450 kg/m3 produced better results than the alternative values tested. The mechanical characteristics of RHA percentage replacement of 10 percent and 30 percent were more useful than FA in each group. The water permeability of all mixes reduced as the cementitious quantity rose due to the reduction in entrapped air. As the cementitious level reduced, the water permeability loss ratios rose. Mater et al. [36] developed an artificial neural network (ANN) model to assess the compression strength of green concrete by combining waste disposal and artificial intelligence (AI).The recommended technology allows for partial replacement of concrete components with recycled coarse aggregate (RCA), recycled fine aggregate (RFA), and fly ash (FA).The model was built, trained, and evaluated in Python using experimental data obtained from the literature. The results showed that replacing 10% FA with cement caused a modest drop in compressive strength of up to 9%, particularly at young ages.

Naseri et al. [37] optimized the green and sustainable concrete mixture proportion. The model that needed to be developed in this example considered concrete functional characteristics (such as fast chloride permeability test, carbonation, and slump, compressive strength), unit cost, and environmental consequences. As a consequence, a novel prediction approach is known as "Marine predator programming" was supplied to the model. ANN, support-vector machines (SVMs), and second polynomial regression were used to evaluate the implementation of the generated ML model. The findings showed that Marine predator programming was extremely capable of estimating many tangible aspects. Eco-friendly combinations can lower the environmental score by 74.37% and 67.83%, respectively. Sustainable mixing proportions have a sustainability rating of up to 80.03% lower than conventional experimental combination proportions. Water absorption, split tensile strength, compression strength, and concrete slump test with varied amounts of rice hull ash as a replacement for cement and fine particles substituted with coal bottom ash (CBA) were separated and blended by Bruskheel et al. [38]. The modifiability and amount of water absorbed by concrete reduced as the amounts of RHA and CBA in concrete increased. Furthermore, applying 5 percent RHA and 30 percent fine aggregate (FAg) in concrete for 4 weeks consistently increased compression strength and split tensile strength by 9.10% and 7.73%, respectively. By partially substituting rice hulls ash as a cementing ingredient from 0 to 40 percent, Patnaik et al. [39] studied the fresh, mechanical, and durability properties of concrete based on C30 grade rice hull ash. The test findings also revealed that as the percentage of OPC substituted with rice hull ash increases, the compression strength and tensile strength of cured concrete increases, before declining. For non-destructive concrete compressive strength

testing, the rebound hammer test was used, and a mathematical relationship was developed between the compression and rebound values of RHA concrete, which showed a strong correlation.

Current studies and allied sectors have started to concentrate on climate change and environmental problems. As a result, numerous methods and indicators have been created to better identify the primary causes of these issues and to take steps to mitigate their effects. For the environmental assessment of "green" concrete mixes, a systematic Life Cycle Assessment (LCA) method is needed. Despite the importance of environmentally friendly infrastructure actions, the rising costs of building materials and other building supplies, and the reality that even before concrete is poured in a structure, its effects are imprinted for several years [40], a life-cycle framework is especially important for a systematic detection and characterization of the environmental impacts of both traditional and "green" concrete production. LCA is a method for statistically and comparably analyzing the environmental effect of a product/process [41]. The use of SCMs instead of clinker/cement has been shown to have a lower environmental effect [17]. Despite various researches focusing on ecologically friendly concrete mixes utilizing FA, the authors are unaware of any LCA of rice hull ash concrete. Rice hull ash in concrete is not widely used in the U.S. since nowadays it is a novel product that requires additional investigation into its environmental implications. Because RHA improves early strength development, which is an issue with FA concrete, it can be used instead of OPC in the concrete mixture [42]. Figure 1 summarized the structural and environmental benefits of using FA and RHA in concrete. The development of intelligent models to optimize the utilization of the combined effect of rice husk ash (RHA) and fly ash (FA) in concrete would have solved the inconsistency in the right proportions to achieve the required strengths for a more sustainable infrastructure. Furthermore, a clearer understanding of the environmental impact of the inclusion of RHA and FA in concrete as partial replacements for cement would have equally informed future research, design, and construction of concrete structures on the optimal amount of replacement needed to achieve sustainable strength without further endangering the environment.

In this study, intelligent models and mix design tools/charts have been proposed for rice husk ash and fly ash blend concrete data points under environmental impact considerations for the hydro-mechanical properties (slump, compressive strength, splitting tensile strength, flexural strength, bonding strength, elastic modulus, and permeability) of concrete.

2. Background Literature Review

2.1. Green Concrete

During the last century, the building and construction industry have relied heavily on concrete, the most frequently utilized and efficient man-made substance [43–47]. Concrete constructions can be customized to have any required qualities and come in just about any required form. This is conceivable due to the robustness, foldability, and less life cycle cost of the material [48–51]. The primary conventional binder for concrete manufacture is Ordinary Portland Cement (OPC). By 2050, cement consumption is predicted to exceed 6 Gt/year [52–54]. OPC manufacture requires a significant amount of fuel and natural resources. It is a multi-stage industrial process that produces massive amounts of greenhouse gases such as CO_2 [55–57]. Numerous environmentalists criticize the manufacturing industry for pollutant emissions, claiming that it contributes for around 5–7% of worldwide CO2 emissions. For every kilogram of cement created, around 0.8-0.9 kg of CO_2 is released [58, 59]. There is worldwide agreement on the need to reduce the carbon footprint of the cement industry via substantial substitution of cement in concrete. As a result, a solution for the long-term sustainability of concrete is required, as is the development of a new binder capable of overcoming the barriers associated with the manufacture and implementation of OPC [60–62].

Supplementary cementitious materials (SCMs) constitute substances that may be used in lieu of OPC in certain situations. Many industrial and agricultural waste products are now being employed as SCMs on a global scale. Fly ash (FA), rice husk ash (RHA), volcanic ash (VA), electric arc furnace slag (EAFS), zeolite (ZLT), metakaolin (MK), and silica fume (SF) are the most frequently utilized SCMs [63, 64]. Different industrial wastes have been employed to enhance the mechanical and durability qualities of concrete throughout the years. This also contributes to reducing reliance on OPC. Among the many types of industrial waste, FA is widely utilized and has been seen as a viable substitute for OPC [65–67]. FA is a coal combustion byproduct that is also collected from coal-fired thermal power plants. It has been used in place of OPC or clinker cement as a partial substitute for a long period of time. The amount of FA in the combination is limited to 15%–20% by weight of the OPC [68–70]. The concrete produced with high-volume FA has such a low per-unit cost of manufacture. Attributed to the prevalence of SiO2 and Al2O3, FA has a unique pozzolana characteristic. SiO2 and Al2O3 combine with calcium hydroxide during the hydration process, generating additional calcium silicate hydrate (CSH) and calcium aluminate hydrate (CAH). The concrete appears to be getting denser when CSH and CAH are present. Additionally, it plugs voids in the concrete and strengthens the matrix. It contributes to the reduction of the difficulties associated with sustainable building, including its environmental effects [71].

Alternatively, it should be mentioned that RHA has grown to become one of the most important SCMs in the world. Among the SCMs derived from rice crop agricultural waste is RHA, which is derived from the waste of the rice crop [72, 73]. Rice grains are wrapped with rice husks (RH), which are then used as a fuel in rice mills to boil the paddy that has been harvested. As a silica-containing material, it has the potential to be utilized effectively as an SCM in the production of concrete [74]. As a result, RHA may be used as a cementitious material with efficiency in certain applications. RHA does not emit a significant quantity of carbon dioxide into the atmosphere. It has the potential to be employed as a structural concrete. Not only does it add to the overall strength of the concrete, but it also contributes to the long-term durability of the concrete's qualities [75].

2.2. Machine Learning Approach

2.2.1. Evolutionary Polynomial Regression (EPR)

Genetic Algorithm (GA) is famous optimization technique depends on simulating the evolution process of biological creatures. It depends on one simple rule "The most fitting creature will survive". To apply this principal on optimization, there must be a pool of solutions for the considered problem, a fitting criterion and a procedure to generate new solutions by mixing the existing ones. Biological creatures transfer their data to the next generation as an arranged series of genes called "Chromosome", similarly, (GA) presents the solution (chromosome) as an arranged list of steps (genes). (EPR) is a direct application of (GA), it depends on optimizing the number of terms of the "Traditional Polynomial Regression (TPR)". (TPR) is a well-known mathematical regression technique uses "Least Squared Error" principal to find the optimum coefficient values of a certain polynomial function to fit a certain dataset. The considered polynomial may be single or multi variables depending on the considered problem configuration (dataset). The chosen polynomial degree (its highest power) depends on the complexity of the considered problem, first degree polynomial (linear) may be used for simple problems, for more complicated ones, second degree (quadratic), third degree (cubic) of higher degrees may be required. The number of polynomial terms dramatically increases with increasing the variable numbers and polynomial degree, for example, a two variables second degree polynomial have only six terms (X2+Y2+ XY+X+Y+C), while three variables third degree polynomial have 20 terms and four variables forth degree polynomial have 70 terms and so on. As the number of polynomial terms increases, it becomes more difficult to apply less practical. Hence, (EPR) technique aims to optimize the (TPR) by eliminating the less important terms and keep only the most effective ones using (GA) technique. So, the population (solutions) consists of a set of polynomials, the fitting criteria is the "Sum of Squared Errors (SSE)" and the chromosome consists of a list of polynomial terms, the length of the chromosome is the chosen number of terms. Cycles after cycle, the most important terms accumulate in the survival chromosomes and the less important ones deleted.

2.2.2. Artificial Neural Network (ANN)

(ANN) is an umbrella of a wide range of (AI) techniques that depends of mimicking the behavior of biological neurons. They all consist of nodes (cells or neurons) and links to connect the nodes, but they have different neurons arrangement and connection patterns. "Multi-Layer Perceptron (MLP)" is one of the earliest and most (ANN) types. It is the commonly used type for regression problems. It consists of a number of nodes arranged in layers, the first layer is called "Input layer" and it is used to receive the input values, while the last layer is called "Output layer" and it is used to deliver outputs values. Between the input and the output layers there are a number of intermediate layers called "Hidden layers", they are responsible of predicting the outputs from the inputs. (MLP) must have one hidden layer at least. Each node in a certain layer is connected to all the nodes in the previous and the next layers by links, but the nodes of each layer are not connected to each other. Each link has an importance factor called "Weight" and each node has a triggering formula called "Activation Function", this could be any nonlinear function, but the most popular ones are the sigmoid, the hyper-tan and the ramp functions, they are responsible of the nonlinear capability of the (ANN). Due to the variation in ranges of input values, all inputs must be scaled to a unified range, this process is called "Standardization" if the input variance is divided by its standard deviation (SD) and called "Normalization" if the inputs are scaled between (0 to 1) and called "Hyper normalization" if the inputs are scaled between (-1 to 1). The scaled inputs propagate from the input layer to the output layer through the hidden layers. The output of certain node is the result of applying its activation function on the summation the node inputs multiplied by corresponding links' weights. After the output layer, the outputs must be de-scaled to its original renege. Any (ANN) model must be trained using a given dataset, during the training process the weight values of the model's links are adjusted to predict the correct outputs from the inputs. There many training techniques could be used to find the optimum values for links' weights such as "Back Propagation (BP)", "Gradually Reduced Gradient (GRG)" and "Genetic Algorithm (GA)".

2.3. Life Cycle Assessment

Climate change is attributed to the increase in greenhouse gas emissions (GHG) in the atmosphere. Approximately 54 giga-tons of carbon dioxide (CO2-eq) were recorded as the total annual GHGs emissions in 2017. Concrete is one of the main contributors to these emissions and concrete usage and demand for cement in the construction industry is

expected to be increased in the future due to the rapid urban development in emerging countries. Annually about 20 billion tons of concrete are produced worldwide, and Portland Cement (PC) production is responsible for 7–10% of total CO2 emissions. When considering the construction and building sector, approximately 80% of the GHG emissions and energy consumption are generated during the operation phase of the buildings. Many studies have been conducted and introduced new technologies, policies, and mitigation measures/techniques to reduce GHG emissions during the operation stages [76]. However, around 10–20% of GHG emission and energy consumption is from material manufacturing, construction, and demolition, with limited studies reported related to reducing GHG emissions and other environmental impacts during material production and construction stages [77]. Life Cycle Assessment (LCA) is an established and well-known method that can evaluate the environmental impacts of products throughout its life cycle. To date, limited studies have been conducted to compare the detailed environmental impact of using blended alkali-activated binders against PC binders in the construction industry. Adapting the waste products (fly ash and RHA) by replacing cement in the construction industry reduces the environmental impact and cost obtained from source material manufacturing and solves problems associated with landfill disposal activities [78, 79]. The utilization of such industrial and agricultural waste could be a massive benefit to the environment. Hence this study investigates the GHG emissions from cradle to end of building construction stage (cradle to end of construction), a life cycle impact and benefit assessment of the manufacturing stage (cradle to gate) and initial cost analysis of fly ash geopolymer concrete (100FA), alkali-activated fly ash-RHA blended concrete (hereafter, used as blended alkali-activated concrete) and comparing with PC concrete. The outcomes of this study will useful when adapting feasible, sustainable alternatives in alkali activated concrete manufacturing and construction considering the environmental and economic aspects [59, 80].

As previously stated, the substitution of OPC with SCMs has long been considered as one of the most efficient methods of reducing greenhouse gas emissions. Additionally, it is essential mentioning that the amount of cement in the mix has a direct correlation with the concrete's durability, environmental impact, quality, and other characteristics. Scholars employed experimental methods to investigate the effect of SCMs on the mechanical properties of green concrete. Pitroda et al. [81] examined the mechanical properties of concrete by varying the fly-ash concentration. The fly-ash content was tested by substituting fly-ash for cement. When the qualities of conventional strength concrete were compared to those of concrete containing 10% fly ash, it was determined that the latter possessed superior properties. Once the fly-ash concentration approached ten percent, the concrete's mechanical properties deteriorated as the fly-ash amount grew. Saha [82] studied the use of class F fly ash as a partly cement replacement in concrete. Compared with the control samples, the fly ash specimens had an exceedingly low early compressive strength. Nonetheless, the pozzolanic activity improved the specimens' strength over time, whereas the reference samples' strength paused after 56 days of curing. Increasing the fly ash content in the mix reduced drying shrinkage. Using fly ash as a binder reduced the porosity of the concrete. As a result, the fly ash concrete's water sorptivity and chloride permeability were lowered. Giaccio & Malhotra and Feldman et al. [83, 84] conducted extensive study on high-volume FA concrete. The experimental findings indicated that concrete containing a high proportion of Class F FA enhanced mechanical qualities, had extremely little chloride ion penetration, exhibits adequate resistance to repeated freezing and thawing cycles, and had no adverse effect when reactive aggregate was added. Bouzoubaâ et al. [85] observed that test results of concrete comprising class C and class F FA were equivalent to or superior to those achieved using ordinary concrete. As a consequence, FA concrete offers equivalent or superior properties in comparison with ordinary concrete while being less costly. Over the course of 28 days, Poon et al. [86] explored the compressive strength of concrete comprising 45% FA and discovered that the concrete attained a compressive strength of 80 MPa and exhibited lesser heat of hydration and chloride diffusivity when compared to OPC. The influence of plastic waste (PW) and graphene nanoplatelets (GNP) on the characteristics of high-volume fly ash (HVFA) concrete was explored by Adamu et al. [68], and the outcomes indicated that the response surface methodology was utilized for experiment design, data modeling, and process optimization. PW, HVFA, and GNP were used as variables, and the materials' strength and water absorption were used as responses. PW and HVFA both diminish strength and absorption, but GNP strengthens both of these features. Each suggested model was statistically substantial and had a high level of correlation [85-87].

Rice husk is among the most common agricultural wastes, obtained from the outer coating of rice grains throughout the milling operation. It is one of the most common crop wastes. Twenty percent of the 500 million tons of paddy produced across the globe comes from this region. More academics have thus concentrated their efforts on the impact of this ecologically friendly substance on the qualities of concrete as a result. For example, in 2005 Bui et al. [64] evaluated the effect of particle size on the strength of blended gap-graded Portland cement concrete made with RHA. This study investigated the strength activity index of mortars including residual RHA created during the burning of rice husk pellets and RHA derived via grinding residual RHA. The compressive strength and durability of concrete were examined when ground RHA was partially substituted for cement. Ameri et al. [87] implemented a study about concrete including RHA. According to the findings, concrete with RHA exhibited a significant increase in early compressive strength. Increases in RHA concentrations greater than 15% resulted in a decrease in compressive strength. This is due to the presence of an overabundance of silica in RHA which was not been reacted with other components. Iqtidar et al. [88] employed machine learning to forecast the qualities of RHA-containing concrete. This research evaluated the compressive strength of rice husk ash mixed concrete using 192 data points. Age, quantity of cement, RHA,

superplasticizer, water, and aggregates were all input factors. This study used four approaches of soft computing and machine learning, including artificial neural networks (ANN), adaptive neuro-fuzzy inference system (ANFIS), multiple nonlinear regression (NLR), and linear regression. The acquired data were evaluated using sensitivity analysis, parametric analysis, and the correlation factor (R2). The findings indicated that ANN and ANFIS outperformed other approaches. Amin et al. [63] employed sophisticated machine learning approaches to estimate the compressive strength of RHA. Six inputs were chosen based on the available literature: specimen age, percentage of rice husk ash, percentage of superplasticizer, aggregates, water, and quantity of cement. The results of machine learning techniques were compared to those of more conventional techniques such as linear and non-linear regressions. The performance of machine learning approaches was shown to be superior to that of conventional methods for calculating the compressive strength of RHA. Iftikhar et al. [89] used machine learning methods to anticipate and establish an empirical formula for the compressive strength of concrete containing RHA. Gene expression programming (GEP) and Random Forest Regression (RFR) were used in this investigation. The models were developed using a dependable database of 192 data points. The most significant factors in the creation of RHA-based concrete models were age, cement, RHA, water, superplasticizer, and aggregate. Models were evaluated using a variety of statistical variables.

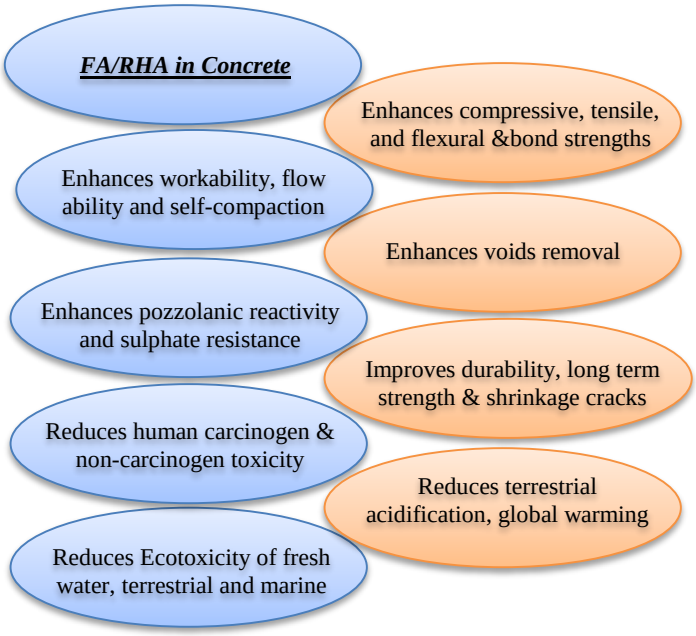

Figure 1. The structural and environmental benefits of FA and RHA in concrete

2.4. Novelty and Innovation

In an effort to propose models; analytical and numerical in order to solve the problems of sustainability in concrete production and also those of repeated visits to laboratories prior to design and construction activities, databases of various sizes have been explored as well as different artificial intelligent techniques. In this present research work, an extensive literature search was done to collect a rich database comprising of concrete constituents, which include rice husk ash (RHA) and fly ash (FA), which form the focus of this work in terms of sustainable concrete devoid of or with less amount of greenhouse emission footprint. Also, these concrete constituents were reduced to ratios, which make easier unlike in previous works to handle and predict more accurate functions. In addition, the evaluation of the environmental impact of the concrete constituents was conducted to determine the life cycle assessment potential, which was incorporated into further research considerations in this work. Moreover, multiple AI techniques have been deployed in this research work to a step further to propose concrete design tools/charts, which works in synergy with the closed-form AI models to predict concrete design mixes of desirable strength and accompanying reduced environmental impact. With all these innovative considerations, this research work stands out from what has been researched previously in this field of sustainable and artificial intelligence applications.

3. Methodology

3.1. Collection of Concrete Experimental Data

An extensive literature study was conducted, which gave rise to multiple points of concrete mixes containing the following; cement, rice husk ash, fly ash, water, plasticizer, fine aggregates, and coarse aggregates [90]. The following concrete hydraulic and mechanical properties were studied; air content, slump, hydraulic conductivity, compressive strength, splitting tensile strength, flexural strength, bonding strength and elastic modulus. In Figure 2, the theoretical framework of the research methodology and modelling operations are presented.

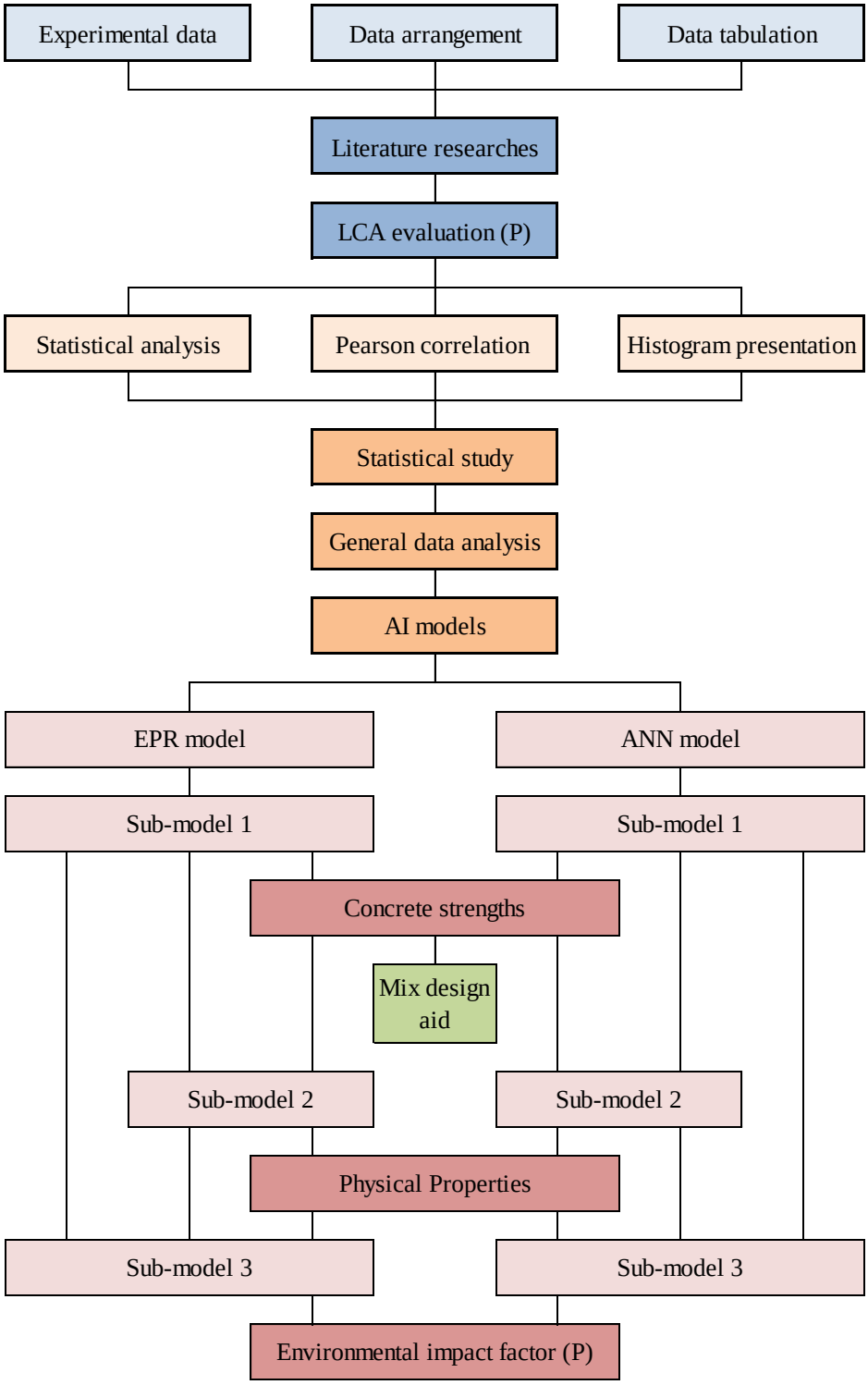

Figure 2. The theoretical framework of the research methodology and modeling

3.2. Collected Database and Statistical Analysis

At the end of the literature study, 105 records were collected for experimental tested concrete mixtures with different components' ratios. Each record contains the following data: cement to binder ratio (C/B), aggregates (coarse plus fine) to binder ratio (Ag/B), super-plasticizer to binder ratio (PL/B), concrete mix slump (S) mm, cylinder compressive strength of concrete after 3, 7, 28, 60 & 90 days (Fc03, Fc07, Fc28, Fc60 & Fc90) MPa, splitting tensile strength after 28 days (Ft28) MPa, flexural tensile strength after 28 days (Ff28) MPa, bond strength after 28 days (Fb28) MPa, modulus of elasticity after 28 days (Ec28) GPa, water permeability after 28 days (K28) pico-meter/sec (10-12 m/sec) and environmental impact factor (P).

Where (B) is binder content (cement content + fly ash or rice husk ash content). For all collected concrete mixes, the additional cementitious material was either fly ash (FA) or rice husk ash (RHA) but not a combination of them. Also,

the ratio between coarse and fine aggregates (CAg/FAg) is constant and equals to 2.0 in all collected design mixes, hence, both of them are equivalent to only one independent variable presented by total aggregate content (Ag). The collected records were divided into training set (85 records) and validation set (20 records). Table 1 includes the complete combinatorial dataset, while Tables 2 and 3 summarize their statistical characteristics and the Pearson correlation matrix. Finally, Figure 3 shows the histograms for both inputs and outputs. This presents the internal consistency of the studied parameters, which shows their distribution frequency in the array of the concrete mix points. It can be observed that C/B and Ag/B have the more central distribution within the central bin of the database for the inputs while S has the most central distribution bin for the outputs.

Table 1. Combinatorial utilized database

C/B (--)	Ag/B (--)	PL/B (--)	S (mm)	Fc03 (MPa)	Fc07 (MPa)	Fc28 (MPa)	Fc60 (MPa)	Fc90 (MPa)	Ft28 (MPa)	Ff28 (MPa)	Fb28 (MPa)	Ec28 (GPa)	K28 (pm/s)	P (--)
Training dataset														
0.68	4.71	0.03	115	36.05	62.43	66.22	96.95	92.51	7.10	10.70	11.18	39.15	4.07	8.38
1.00	5.10	0.00	85	12.40	23.30	31.10	32.90	34.50	3.10	4.50	5.00	22.40	8.50	6.36
1.00	4.10	0.03	90	37.10	55.20	73.50	78.60	82.30	6.70	10.80	12.20	41.00	5.20	8.90
0.66	4.01	0.03	104	40.28	53.22	86.79	73.60	101.78	7.85	11.83	11.14	36.38	3.17	3.48
0.90	3.32	0.03	110	45.10	65.60	86.80	93.80	98.10	7.70	12.80	14.40	43.90	4.20	8.95
0.90	2.83	0.03	119	47.41	75.65	82.63	89.01	116.96	7.83	15.26	13.55	52.21	3.81	11.40
0.70	4.72	0.00	66	11.74	21.54	27.29	35.23	31.86	2.91	4.75	4.47	21.71	4.85	2.69
1.00	4.80	0.00	74	11.28	23.07	32.34	33.56	38.64	2.91	4.68	5.00	19.04	8.93	6.53
0.88	5.66	0.00	76	16.07	28.30	30.71	41.03	36.36	3.16	4.60	6.16	21.84	5.55	6.15
0.79	4.44	0.03	124	48.92	71.28	81.87	97.14	84.91	9.09	11.35	12.33	39.25	3.76	5.30
0.70	3.32	0.03	127	46.27	66.10	77.16	81.52	100.88	8.14	11.74	15.88	45.22	2.70	10.90
0.82	4.68	0.00	80	15.84	26.90	35.70	42.07	36.52	3.40	5.41	5.30	29.04	5.19	4.41
0.89	4.51	0.03	92	40.28	76.95	80.37	104.31	87.09	8.10	11.66	12.58	47.57	4.10	6.83
0.66	4.26	0.03	128	42.33	68.77	78.90	75.29	88.50	7.20	12.76	11.92	44.84	3.49	3.37
1.00	3.62	0.03	96	31.91	55.20	72.03	75.46	75.72	5.96	10.58	14.03	45.10	5.67	9.77
0.80	4.13	0.03	110	45.30	66.00	87.10	93.40	97.60	7.90	12.90	14.50	44.10	3.80	5.65
0.79	4.52	0.03	94	49.83	66.66	92.33	103.67	85.89	6.72	13.93	13.49	44.54	4.14	5.18
0.67	5.50	0.00	68	11.39	24.38	27.26	38.99	36.57	2.88	5.20	4.34	23.94	5.20	6.07
0.70	2.78	0.03	132	53.42	62.80	96.24	87.14	85.05	6.19	13.80	14.70	41.71	2.76	12.10
0.89	5.45	0.00	72	12.92	25.10	42.38	39.80	47.96	3.96	5.28	5.58	27.81	6.22	4.72
0.64	4.40	0.03	136	45.36	57.72	86.47	79.24	100.43	6.67	10.01	14.56	42.94	3.57	8.94
0.77	3.15	0.03	103	51.31	61.42	97.73	100.60	100.03	6.62	12.33	17.58	52.67	2.94	5.94
0.70	3.38	0.03	150	50.02	59.45	81.10	101.84	112.40	6.72	11.70	13.17	45.39	2.67	4.50
0.69	3.36	0.03	122	41.50	62.13	78.03	104.01	91.98	7.78	14.71	15.88	39.95	3.33	10.70
0.80	5.13	0.00	75	14.60	27.20	36.10	38.80	40.50	3.50	5.30	5.80	26.00	5.50	6.52
0.88	3.66	0.03	106	46.45	57.73	97.22	90.05	106.93	8.09	13.57	12.38	47.85	3.70	8.00
0.73	3.98	0.03	127	42.12	63.02	72.45	93.57	81.05	6.46	10.47	13.52	45.47	4.26	9.52
0.70	3.75	0.03	112	45.70	68.80	78.48	99.02	90.71	7.67	11.96	16.58	43.17	2.38	4.12
0.89	5.06	0.00	79	14.59	25.38	39.38	41.79	46.70	3.96	6.27	5.10	28.08	5.38	4.82
0.75	4.07	0.03	112	42.33	55.61	84.42	82.06	95.58	7.99	12.30	13.62	44.42	3.46	4.92
0.90	3.10	0.03	120	49.90	69.40	90.80	98.90	103.50	7.60	13.50	15.40	45.40	3.40	10.90
0.89	5.36	0.00	68	13.07	25.38	38.25	35.42	35.86	3.85	4.90	5.46	23.49	5.54	4.95
1.00	3.09	0.03	95	43.00	61.10	80.80	87.20	91.20	6.90	11.90	13.70	42.40	4.20	10.80
0.83	2.97	0.03	115	43.69	71.31	97.73	104.58	105.24	6.78	14.80	13.35	50.84	2.55	7.69
0.91	2.79	0.03	121	45.85	82.15	101.33	110.59	111.28	6.87	15.93	16.10	41.39	2.58	9.56
0.72	5.12	0.00	68	12.03	27.01	30.12	34.92	36.57	3.32	4.37	5.10	25.76	5.30	6.81
0.90	3.05	0.03	121	39.24	61.01	80.72	90.05	95.16	6.85	14.59	13.10	39.07	3.95	9.77
0.80	3.84	0.03	115	48.79	72.49	100.21	81.79	104.37	7.44	11.31	14.75	42.02	3.88	9.47
0.81	4.58	0.00	71	15.62	29.65	40.43	42.68	35.24	3.54	6.10	6.21	25.48	5.83	7.14
0.90	3.87	0.03	99	51.86	62.78	83.94	89.96	89.09	7.53	14.41	13.32	43.94	4.45	7.87

0.82	4.90	0.00	73	13.54	24.48	36.77	33.73	41.29	3.82	5.62	6.50	25.70	5.83	4.16
0.76	3.42	0.03	118	45.99	75.05	101.26	89.14	109.08	8.97	12.42	17.06	47.02	2.91	10.50
0.67	3.42	0.03	153	40.55	66.76	98.84	98.39	88.02	6.34	14.06	12.64	46.53	2.88	10.60
0.90	3.10	0.03	115	52.10	72.70	94.70	102.40	107.00	7.90	14.10	16.10	46.50	3.00	8.79
0.89	3.31	0.03	123	57.31	67.61	82.39	94.21	107.00	8.06	13.82	14.81	51.62	2.91	8.34
0.88	5.38	0.00	82	17.18	31.02	39.75	42.98	42.12	3.70	5.50	5.10	23.76	4.93	4.79
0.90	5.13	0.00	75	15.20	28.20	37.50	39.80	41.70	3.70	5.50	6.00	27.00	5.60	5.10
0.80	4.12	0.03	115	45.60	66.50	87.90	95.10	99.40	8.00	13.00	14.60	44.70	4.00	9.11
0.73	4.93	0.00	73	11.26	24.62	36.14	37.63	37.28	2.82	4.46	5.25	25.54	5.05	6.54
0.70	4.14	0.03	115	41.10	59.80	78.90	84.60	88.50	7.20	11.60	13.10	42.30	3.60	4.03
0.91	4.40	0.00	87	14.24	24.89	39.44	35.06	40.66	3.71	5.35	6.05	28.11	6.02	7.17
1.00	2.99	0.03	101	44.72	67.21	70.30	77.61	82.08	7.73	11.31	15.62	41.55	3.86	11.20
1.00	4.56	0.03	100	40.07	57.41	72.03	70.74	74.89	6.03	10.58	10.49	41.00	5.30	8.32
0.79	3.06	0.03	113	58.25	70.09	99.40	104.34	103.78	8.27	13.11	13.90	52.55	2.70	10.90
0.70	2.72	0.03	137	46.18	73.48	82.84	80.16	85.78	6.79	11.18	15.39	41.39	2.73	5.36
1.00	2.69	0.03	84	36.98	66.60	71.91	92.43	91.20	5.87	13.45	15.48	43.25	3.57	11.90
0.78	4.61	0.03	102	48.34	57.19	80.87	97.00	109.34	9.04	14.43	12.85	45.59	3.88	8.27
0.90	2.94	0.03	112	48.40	61.77	97.16	112.75	104.54	6.84	13.64	16.94	43.13	3.57	11.10
0.64	5.57	0.00	68	13.16	21.78	33.38	34.20	34.01	3.14	4.61	4.73	20.56	4.80	1.68
1.00	3.12	0.03	98	38.70	64.77	82.42	95.05	78.43	7.80	13.45	14.25	36.89	4.79	10.80
0.80	4.84	0.03	99	45.14	73.15	77.35	83.69	88.47	7.04	13.26	14.16	39.78	4.60	7.94
0.82	4.81	0.00	69	12.67	29.86	37.84	40.17	34.54	3.64	4.78	6.50	22.87	5.19	4.39
1.00	4.00	0.03	100	37.47	49.68	69.83	88.82	86.42	7.71	9.18	12.08	35.67	5.30	9.18
0.80	4.58	0.00	67	14.75	31.28	38.63	38.02	35.64	3.57	5.14	5.92	23.92	6.22	7.11
0.80	4.71	0.03	104	45.14	72.49	81.75	101.76	109.34	8.32	12.22	12.99	48.72	3.96	8.34
0.70	4.57	0.00	62	13.57	24.14	34.55	29.49	37.99	2.91	5.24	5.61	24.85	4.85	7.49
0.68	3.19	0.03	129	54.35	58.78	97.66	87.70	107.47	7.15	13.65	13.47	41.83	2.43	4.48
0.92	3.20	0.03	109	44.65	64.29	77.25	97.55	106.93	6.85	10.88	15.41	37.75	4.79	9.34
0.70	5.14	0.00	70	12.80	23.90	31.70	33.90	35.50	3.10	4.60	5.10	22.80	5.10	6.61
0.70	4.13	0.03	120	40.50	58.90	77.90	84.30	88.10	7.10	11.50	13.00	42.10	3.80	9.22
0.82	3.12	0.03	133	51.31	62.13	83.90	93.62	107.33	6.55	11.65	16.96	48.55	2.66	7.09
0.79	3.22	0.03	104	43.69	74.13	83.90	101.59	103.16	7.24	15.76	17.11	52.21	3.11	6.64
0.70	3.12	0.03	130	48.10	66.80	87.20	94.30	98.60	7.30	13.00	14.80	44.50	2.70	4.82
0.81	2.78	0.03	124	49.06	67.26	90.11	96.24	100.61	7.80	15.59	16.12	49.33	2.70	12.10
0.70	3.11	0.03	135	47.70	66.10	86.70	93.70	98.90	7.20	12.90	14.70	43.90	3.00	11.20
0.90	3.57	0.03	127	44.81	75.61	82.39	103.42	99.51	8.85	12.13	16.26	40.92	3.36	7.73
0.88	3.63	0.03	121	51.40	67.32	86.26	87.03	90.05	7.07	12.42	14.32	44.49	3.06	9.92
0.89	4.20	0.03	107	50.96	74.78	91.14	90.05	90.25	8.70	11.78	12.82	49.17	4.83	7.83
0.78	5.60	0.00	65	13.29	28.56	38.99	36.08	42.12	3.68	6.04	6.03	22.36	5.50	6.22
0.90	5.04	0.03	92	39.82	68.85	92.87	105.27	100.10	8.83	12.84	14.95	45.75	3.90	6.22
Validation dataset														
0.90	4.12	0.03	100	46.30	67.50	89.30	95.70	100.10	8.10	13.10	14.80	45.30	3.90	7.28
1.00	4.60	0.03	84	34.87	51.34	63.21	83.32	75.72	6.90	9.83	11.83	36.49	5.36	8.00
0.67	4.29	0.03	133	40.91	51.24	77.12	77.56	98.67	6.46	10.24	13.39	46.31	4.18	8.89
0.88	3.37	0.03	125	53.39	74.26	79.00	91.98	92.12	7.45	14.99	15.55	47.22	3.91	10.40
0.80	4.23	0.03	94	41.22	69.30	80.13	99.00	105.41	7.43	12.64	15.81	48.07	4.10	5.71
0.82	2.98	0.03	136	46.50	80.71	92.90	111.43	98.49	7.57	13.94	14.54	52.09	2.73	11.10
0.89	4.77	0.00	90	15.09	23.58	32.46	38.79	42.23	3.16	5.60	6.33	23.09	6.43	6.62
1.00	5.09	0.00	82	11.78	24.93	32.66	34.87	31.40	2.85	4.77	4.75	24.19	8.59	6.29
1.00	3.68	0.03	90	42.57	69.04	84.03	82.84	92.11	7.94	10.95	12.74	39.86	4.28	9.55
0.70	4.65	0.00	62	10.97	25.17	34.35	31.12	33.65	2.78	4.23	5.67	21.25	4.85	2.71
1.00	5.49	0.00	89	13.76	20.27	32.66	28.95	31.74	3.04	3.87	4.75	19.26	8.50	5.87

0.80	3.11	0.03	120	50.80	70.60	92.20	99.60	104.20	7.70	13.70	15.70	45.80	2.80	6.81
0.70	5.15	0.00	65	12.90	24.20	32.10	34.20	35.80	3.20	4.70	5.20	23.10	4.80	2.57
0.75	3.90	0.03	114	38.63	54.42	69.43	82.91	83.19	7.42	12.99	11.40	36.38	4.07	5.23
0.80	5.21	0.00	67	13.82	29.86	40.34	33.35	35.73	3.01	5.82	5.07	26.21	5.30	3.69
0.89	5.31	0.00	88	11.99	27.51	32.11	36.93	37.54	3.91	5.20	5.77	27.11	5.78	6.43
0.89	2.99	0.03	102	57.31	73.43	90.91	105.47	119.84	9.09	14.10	18.19	40.46	3.03	8.92
0.80	3.11	0.03	125	51.10	70.80	92.90	101.30	105.90	7.80	13.80	15.80	46.10	3.10	11.00
0.81	4.35	0.03	117	49.83	69.96	79.26	85.93	94.67	7.19	12.90	14.79	40.57	4.14	5.65
0.90	5.12	0.00	80	14.10	26.20	34.90	37.30	39.10	3.40	5.00	5.60	25.10	5.90	6.44
0.75	4.95	0.00	57	13.42	25.65	30.50	36.59	32.94	3.39	5.17	4.52	25.64	5.23	3.40
0.89	4.35	0.03	87	39.82	72.23	92.87	91.87	96.10	7.21	11.79	12.58	45.75	3.78	6.77
0.80	5.14	0.00	70	14.40	26.90	35.70	37.90	39.70	3.50	5.20	5.70	25.70	5.30	3.83
1.00	5.26	0.00	98	14.01	26.56	30.79	29.61	29.33	2.73	4.01	5.15	19.71	9.52	6.37
0.83	4.42	0.00	69	15.04	27.20	36.46	41.90	38.07	3.71	4.66	5.45	29.64	4.90	7.11

Table 2. Statistical analysis of collected database

	Mean	Median	Mode	S.D.	Variance	Skewness	Kurtosis	Range	Minimum	Maximum
C/B	0.83	0.81	1.00	0.11	0.01	0.11	-0.98	0.36	0.64	1.00
Ag/B	4.12	4.14	3.11	0.86	0.73	-0.02	-1.28	2.97	2.69	5.66
PL/B	0.02	0.03	0.03	0.01	0.00	-0.72	-1.51	0.03	0.00	0.03
S	100.30	101.00	115.00	23.12	534.6	-0.01	-0.99	96.00	57.00	153.00
Fc03	34.83	41.10	39.82	15.80	249.7	-0.47	-1.47	47.28	10.97	58.25
Fc07	52.59	61.10	25.38	19.88	395.2	-0.47	-1.47	61.88	20.27	82.15
Fc28	68.04	78.90	32.66	24.80	614.9	-0.47	-1.43	74.07	27.26	101.33
Fc60	73.86	84.60	90.05	27.74	769.3	-0.49	-1.46	83.80	28.95	112.75
Fc90	76.71	88.50	36.57	29.26	856.1	-0.49	-1.46	90.51	29.33	119.84
Ft28	6.08	6.85	2.91	2.05	4.22	-0.46	-1.38	6.36	2.73	9.09
Ff28	10.13	11.65	5.20	3.84	14.71	-0.42	-1.43	12.06	3.87	15.93
Fb28	11.32	13.00	5.10	4.41	19.48	-0.43	-1.44	13.85	4.34	18.19
Ec28	37.55	41.39	25.70	10.11	102.1	-0.44	-1.27	33.63	19.04	52.67
K28	4.40	4.10	5.30	1.44	2.09	1.24	2.19	7.14	2.38	9.52
P	7.33	7.11	10.90	2.50	6.27	0.02	-0.82	10.42	1.68	12.10

Table 3. Pearson correlation matrix

	C/B	Ag/B	PL/B	S	Fc03	Fc07	Fc28	Fc60	Fc90	Ft28	Ff28	Fb28	Ec28	K28	P
C/B	1.00														
Ag/B	-0.02	1.00													
PL/B	-0.03	-0.75	1.00												
S	-0.21	-0.73	0.80	1.00											
Fc03	-0.05	-0.80	0.95	0.83	1.00										
Fc07	0.00	-0.78	0.94	0.79	0.95	1.00									
Fc28	-0.06	-0.80	0.94	0.81	0.96	0.95	1.00								
Fc60	-0.01	-0.78	0.94	0.78	0.94	0.96	0.95	1.00							
Fc90	-0.06	-0.79	0.95	0.81	0.96	0.94	0.96	0.95	1.00						
Ft28	0.00	-0.70	0.95	0.74	0.93	0.94	0.92	0.93	0.94	1.00					
Ff28	-0.03	-0.81	0.94	0.79	0.94	0.94	0.95	0.95	0.95	0.91	1.00				
Fb28	-0.01	-0.84	0.94	0.79	0.95	0.95	0.94	0.95	0.95	0.91	0.93	1.00			
Ec28	-0.06	-0.77	0.92	0.78	0.93	0.93	0.93	0.93	0.94	0.90	0.92	0.91	1.00		
K28	0.45	0.72	-0.72	-0.66	-0.78	-0.76	-0.78	-0.77	-0.78	-0.73	-0.78	-0.77	-0.78	1.00	
P	0.30	-0.63	0.54	0.49	0.53	0.55	0.53	0.54	0.52	0.49	0.55	0.57	0.53	-0.31	1.00

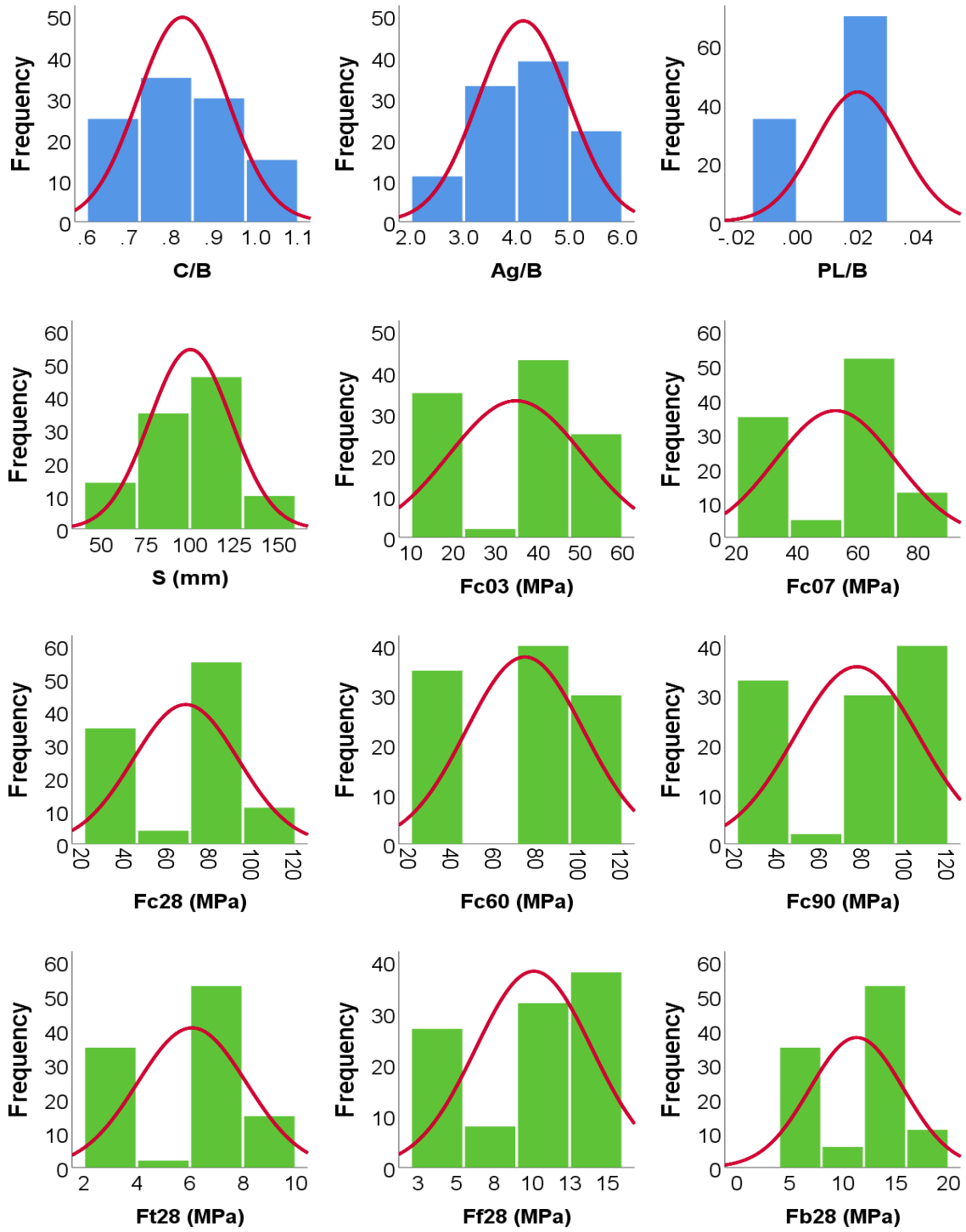

Figure 3. Distribution histograms for inputs (in blue) and outputs (in green)

3.3. Research Program

Two different models were used to predict the twelve outputs of concrete mix using the gathered dataset. The implemented techniques are "Artificial Neural Network (ANN)" and "Evolutionary Polynomial Regression (EPR)". Each implemented technique is based on different approach mimicking human brain for ANN, optimization of mathematical regression for EPR and simulating evolution of natural creatures for GA. However, for all techniques, their accuracies were evaluated in terms of "Sum of Squared Errors (SSE)", "Root of Mean of Squared Errors (RMSE)" and "Determination Coefficient (R^2)".

The values listed in Table 2 illustrated the different correlations between considering inputs and outputs, based on these values the predicting models were constructed as shown in Figure 4. Where the concrete strengths (Fc03, Fc07, Fc28, Fc60, Fc90, Ft28, Ff28 & Fb28) were predicted using the design mix ratios (C/B), (Ag/B) & (PL/B), while the predicted Fc28 is used besides the design mix ratios to predict the values of (S, Ec28 & K28). Finally, the predicted

Fc28, S, Ec28 in addition to the design mix ratios are used to predict (P) values. The next sections present the results of each technique and its accuracy metrics.

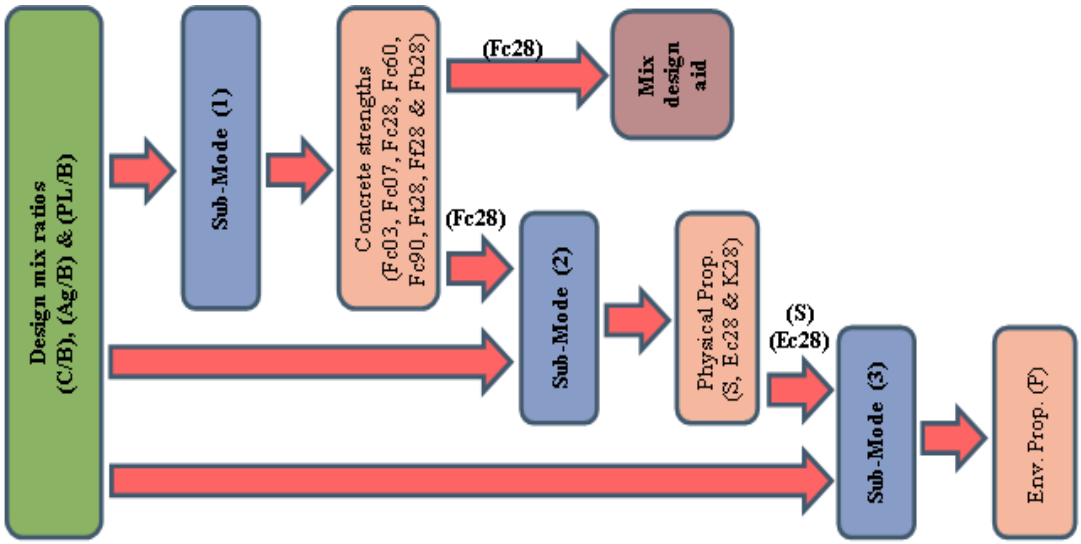

Figure 4. Theoretical framework for concrete design mix and models development and predicting

4. Results and Discussions

4.1. General Remarks on the Concrete Mixes' Strength and Environmental Impact

The concrete mixes collected from literature was reduced to the following ratios; cement to binder (cement + fly ash + rice husk ash) ratio (C/B), aggregate (FAg + CAg) to binder ratio (Ag/B), and plasticizer to binder ratio (PL/B) and the behaviour of the hydro-mechanical properties of the concrete were observed under life cycle assessment (P) considerations. It can be observed that none of the concrete constituents' ratios reacted independent of the other. But more emphasis is placed on the binders and their ratios (C/B and PL/B) as they constitute the contribution to the global warming potential (GWP) of cement use in concrete production, transportation and utilization during construction activities. It is observed that a reduction in the C/B ratio brings about an equivalent reduction in P, though it is not consistent with all the points of the database. This indicates that there is a portion of environmental impact contribution from the Ag/B ratio [35, 85]. This further implies that aggregates (Ag) equally consume energy and release considerable amount of greenhouse emission during the production process (quarrying) and transportation. However, closed-form equations, intelligent models and intelligent mix design tools have been proposed for fly ash/rice husk ash blend in concrete to solve this optimal materials selection and sampling riddles. Furthermore, this development can be employed to solve infrastructural design and problems dealing with concrete structures as well as concrete containment liner systems which need a compressive strength as low as 0.2MPa and hydraulic conductivity (k) of 1E-09m/s for singles liner systems and 1E-07 for double liner systems [25]. It can also be noted that air content was not considered in the parametric study and the models' execution. This was because voids have minor effect on concrete strength, for normal weight, non-air-entrained concrete; the void ratio is ranged between 0.5% and 2.5% with average value of 1.5+/-1%, that affect the strength by +/-5% as per ACI-212 and E4-12.

4.2. Prediction of Outputs

4.2.1. Using ANN Technique

As shown in Figure 4, the predictive model consists of three sub-models. The first is for concrete strengths; the second is for concrete physical properties; and the third is for environmental impact factor. The three sub-models were developed using the ANN technique with a layout of (3:8:8), (4:8:3), and (6:8:1), respectively. All the sub-models used the traditional "Back Propagation (BP)" training algorithm, standardization method (Var/S.D.), and activation function (Hyper Tan). The used network layout is illustrated in Figures 5 to 7, while the weight matrices of each model are shown in Tables 4 to 6. The prediction error % values of the first sub-models were ranged between 6.9% and 9.4% with an average value of 8.2%, and the error % of the second sub-model were ranged between 5.9% and 7.6% with an average value of 7.0%, while the error % of the third sub-model was 6.8%. On the other hand, the R^2 values of the first sub-model were ranged between 0.925 and 0.965 with an average value of 0.945, and for the second sub-model, the R^2 values were ranged between 0.878 and 0.949 with an average value of 0.894, and finally, the R^2 value of the third sub-model was 0.960. This compares well with previous research works which utilized fly ash-silica combination and fly ash alone in concrete production [91-96], and had used other intelligent methods in their prediction of the concrete mechanical properties.

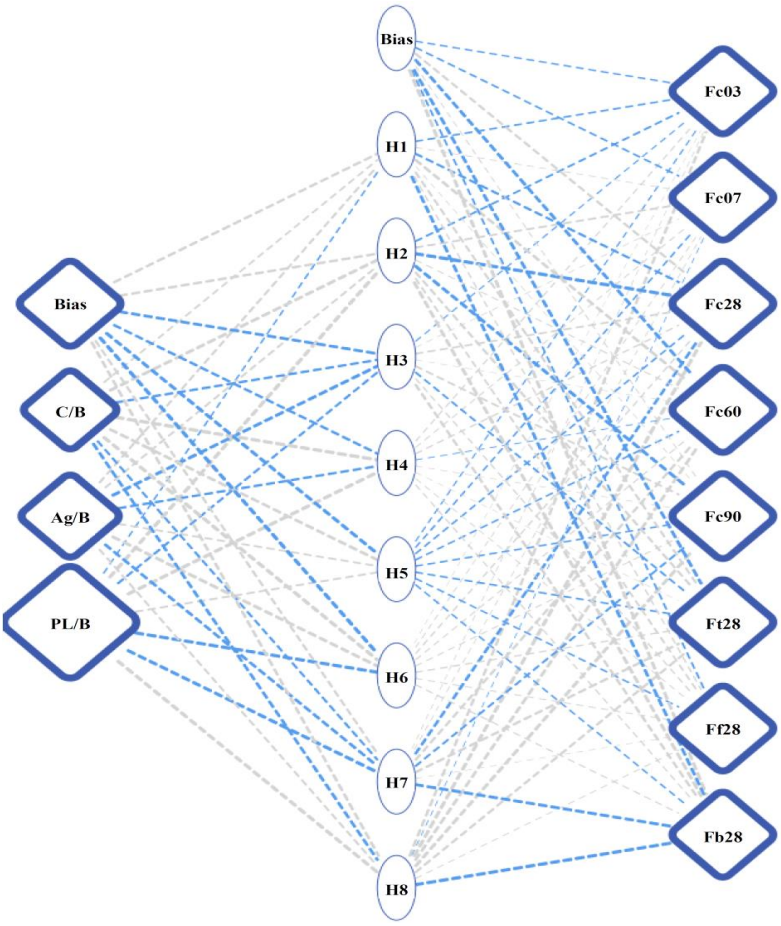

Figure 5. Structure layout for sub-model (1) to predict concrete strengths

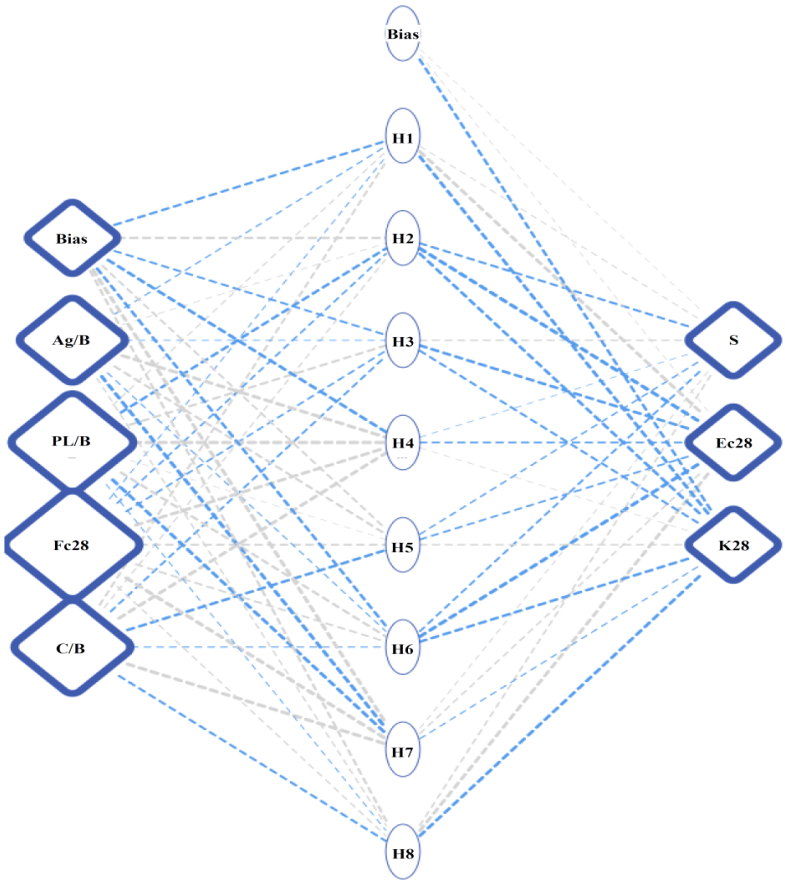

Figure 6. Structure layout for sub-model (2) to predict concrete physical properties

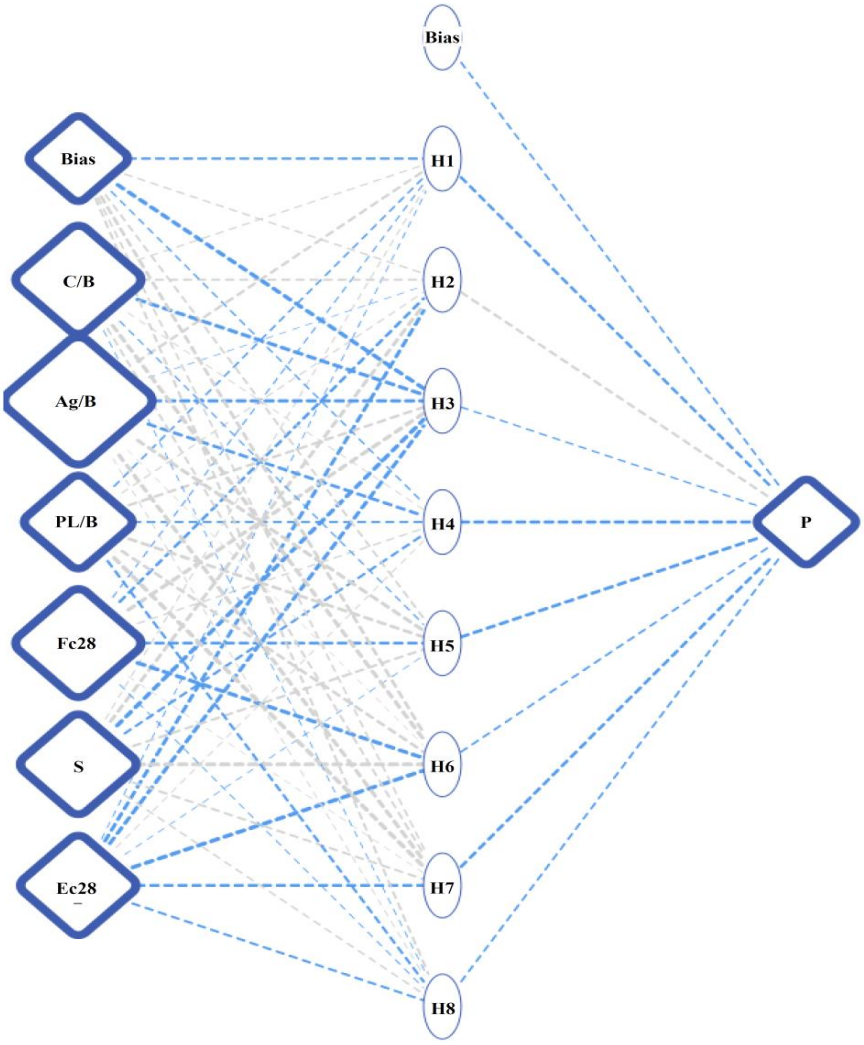

Figure 7. Structure layout for sub-model (3) to predict the environmental impact factor

Table 4. Weights matrix for the developed sub-model (1)

		Hidden Layer								
		H1	**H2**	**H3**	**H4**	**H5**	**H6**	**H7**	**H8**	
Inputs	**Bias**	1.66	1.70	-2.61	-1.59	-4.07	-5.80	1.47	1.99	
	C/B	0.74	3.91	-1.54	10.34	2.70	9.90	-1.10	-2.12	
	Ag/B	1.11	0.93	-3.63	-1.55	0.88	4.91	-2.21	0.96	
	PL/B	-0.34	9.26	-1.20	11.06	0.94	-5.67	-5.39	6.68	
		Hidden Layer								
		H1	**H2**	**H3**	**H4**	**H5**	**H6**	**H7**	**H8**	**Bias**
Outputs	**Fc03**	-0.57	-0.78	-0.25	0.26	-0.26	0.01	0.08	1.56	-0.37
	Fc07	0.09	0.94	0.08	0.16	-0.42	0.14	0.09	-0.06	-0.63
	Fc28	-1.33	-6.01	0.78	0.33	-0.55	0.30	-1.62	5.11	1.39
	Fc60	2.02	0.19	0.05	-0.10	-0.54	0.20	1.47	2.48	-2.60
	Fc90	0.07	-3.59	0.89	0.05	-0.46	0.17	-0.90	3.63	0.14
	Ft28	1.07	1.21	-0.76	0.03	-0.61	0.31	1.57	1.48	-2.51
	Ff28	0.29	0.72	0.30	0.10	-0.45	0.15	0.05	0.15	-0.65
	Fb28	-2.39	3.01	1.53	0.27	-0.41	0.26	-3.21	-5.56	3.09

Table 5. Weights matrix for the developed sub-model (2)

		Hidden Layer								
		H1	**H2**	**H3**	**H4**	**H5**	**H6**	**H7**	**H8**	
Inputs	**Bias**	-1.41	1.70	-0.99	-3.24	0.78	-1.74	5.63	1.18	
	C/B	0.83	0.33	-0.66	6.94	-2.39	-0.23	9.43	-1.07	
	Ag/B	-0.25	0.15	-0.13	8.32	1.28	-0.22	-5.07	0.39	
	PL/B	0.31	-1.88	1.36	10.16	0.09	1.45	-4.11	-0.16	
	Fc28	-0.18	-0.49	-0.51	5.24	1.00	0.78	10.89	0.39	
		Hidden Layer								
		H1	**H2**	**H3**	**H4**	**H5**	**H6**	**H7**	**H8**	**Bias**
Outputs	**S**	0.20	-1.12	0.41	-0.06	-0.41	-0.66	0.18	0.45	0.08
	Ec28	4.15	-8.99	-2.41	-0.55	-0.63	-6.95	0.43	3.50	0.10
	K28	-3.11	-2.38	-1.02	0.13	0.47	-2.11	-0.25	-3.00	-1.64

Table 6. Weights matrix for the developed sub-model (3)

		Hidden Layer								
		H1	**H2**	**H3**	**H4**	**H5**	**H6**	**H7**	**H8**	
Inputs	**Bias**	-2.32	1.24	-10.05	-1.11	1.59	2.73	1.44	1.76	
	C/B	1.06	1.69	-5.68	0.40	-0.79	7.84	1.62	-0.27	
	Ag/B	2.48	-0.04	-4.41	-2.87	3.77	0.04	7.32	0.39	
	PL/B	-1.24	0.94	2.55	-1.56	2.89	2.67	16.07	-2.18	
	Fc28	-0.61	-2.57	8.47	1.15	-2.76	-8.81	0.24	-0.38	
	S	0.75	3.26	-11.13	-2.05	2.37	12.36	1.87	1.34	
	Ec28	-0.38	-3.53	-5.13	0.56	-0.11	-12.45	-2.61	-1.77	
		Hidden Layer								
		H1	**H2**	**H3**	**H4**	**H5**	**H6**	**H7**	**H8**	**Bias**
Outputs	**P**	-2.55	2.43	-1.14	-3.59	-3.06	-1.49	-2.73	-1.50	-1.48

Figure 8 illustrates the relative importance values of each input parameter for P and it indicates that all input parameters have almost the same importance level except (Ag/B) which has a slightly higher importance. This conclusion confirms the proposed theoretical framework shown in Figure 4.

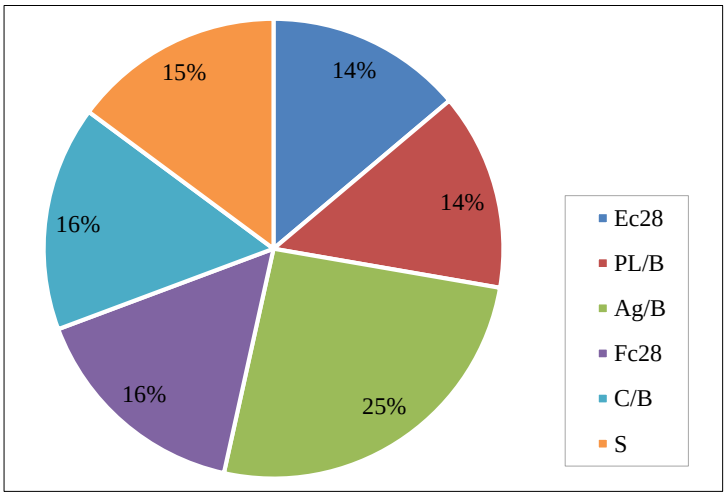

Figure 8. Relative importance of input parameters for (P)

4.2.2. Using EPR Technique

Similarly, the developed EPR model was divided into three sub-models as per Figure 4. The first sub-model was concerned in predicting the concrete strengths using a set of eight optimized cubic polynomials. All polynomials have the same three inputs (C/B, Ag/B & PL/B), hence, each polynomial have 20 possible terms (10+6+3+1=20) as follows:

$$\sum_{i=1}^{i=3}\sum_{j=1}^{j=3}\sum_{k=1}^{k=3} X_i.X_j.X_k + \sum_{i=1}^{i=3}\sum_{j=1}^{j=3} X_i.X_j + \sum_{i=1}^{i=3} X_i + C \quad (1)$$

GA technique was applied on these polynomials to select the most effective five terms of each polynomial to predict (Fc03, Fc07, Fc28, Fc60, Fc90, Ft28, Ff28 and Fb28). The outputs are illustrated in Equations 2 to 9 and its fitness is shown in Figure 9. The error% values were ranged between 9.2% and 10.9% with average value of 9.7%, while (R^2) values were ranged between 0.917 and 0.938 with average value of 0.928. This also compares well with previous research works, which utilized fly ash-silica fume combination and fly ash alone in concrete production [91, 96], and had used other intelligent methods in their prediction of the concrete mechanical properties.

$$\text{Fc03} = 13.8 - 7785\left(\frac{C}{B}\right)\left(\frac{PL}{B}\right) - 5000\left(\frac{B}{C}\right)\left(\frac{PL}{B}\right) - 131\left(\frac{Ag}{B}\right)\left(\frac{PL}{B}\right) + 14100\left(\frac{PL}{B}\right) \quad (2)$$

$$\text{Fc07} = 26.2 - 10280\left(\frac{C}{B}\right)\left(\frac{PL}{B}\right) - 6960\left(\frac{B}{C}\right)\left(\frac{PL}{B}\right) + 1595\left(\frac{B}{Ag}\right)\left(\frac{PL}{B}\right) + 17915\left(\frac{PL}{B}\right) \quad (3)$$

$$\text{Fc28} = -241 + 612\left(\frac{C}{B}\right) - 356\left(\frac{C}{B}\right)^2 + 73\left(\frac{B}{C}\right)\left(\frac{B}{Ag}\right) + 1378\left(\frac{PL}{B}\right) \quad (4)$$

$$\text{Fc60} = -233 + 656\left(\frac{C}{B}\right) - 395\left(\frac{C}{B}\right)^2 + 4132\left(\frac{PL}{B}\right) - 74600\left(\frac{PL}{B}\right)^2 \quad (5)$$

$$\text{Fc90} = 21 + 101\left(\frac{C}{B}\right)\left(\frac{B}{Ag}\right) - 14240\left(\frac{C}{B}\right)\left(\frac{PL}{B}\right) - 8486\left(\frac{B}{C}\right)\left(\frac{PL}{B}\right) + 23905\left(\frac{PL}{B}\right) \quad (6)$$

$$\text{Ft28} = -18.1 + 52\left(\frac{C}{B}\right) - 31\left(\frac{C}{B}\right)^2 + 0.5\left(\frac{B}{C}\right)\left(\frac{PL}{B}\right) + 135\left(\frac{PL}{B}\right) \quad (7)$$

$$\text{Ff28} = -35.4 + 100\left(\frac{C}{B}\right) - 60\left(\frac{C}{B}\right)^2 + 12.5\left(\frac{Ag}{B}\right)\left(\frac{PL}{B}\right) + 730\left(\frac{B}{Ag}\right)\left(\frac{PL}{B}\right) \quad (8)$$

$$\text{Fb28} = 1.2 - 158\left(\frac{C}{B}\right)\left(\frac{B}{Ag}\right) - 106\left(\frac{B}{C}\right)\left(\frac{B}{Ag}\right) + 283\left(\frac{B}{Ag}\right) + 230\left(\frac{PL}{B}\right) \quad (9)$$

The second sub-model was concerned in predicting the physical properties of concrete using a set of three optimized cubic polynomials. All polynomials have the same four inputs (C/B, Ag/B, PL/B & Fc28), hence, each polynomial have 35 possible terms (20+10+4+1=35) as follows:

$$\sum_{i=1}^{i=4}\sum_{j=1}^{j=4}\sum_{k=1}^{k=4} X_i.X_j.X_k + \sum_{i=1}^{i=4}\sum_{j=1}^{j=4} X_i.X_j + \sum_{i=1}^{i=4} X_i + C \quad (10)$$

GA technique was applied on these polynomials to select the most effective seven terms of each polynomial to predict (S, Ec28 & K28). The outputs are illustrated in Equations 11 to 13 and its fitness is shown in Figure 9. The error % values were ranged between 8.6% and 10.5% with average value of 9.3%, while R^2 values were ranged between 0.831& 0.887 with average value of 0.868.

$$\text{S} = 22 + 42\left(\frac{C}{B}\right) + 4.2\left(\frac{C}{B}\right)\left(\frac{Ag}{B}\right) - 5015\left(\frac{C}{B}\right)\left(\frac{PL}{B}\right) - 465\left(\frac{Ag}{B}\right)\left(\frac{PL}{B}\right) + 8570\left(\frac{PL}{B}\right) - 41510\left(\frac{PL}{B}\right)^2 \quad (11)$$

$$\text{Ec28} = -333 + 570\left(\frac{C}{B}\right) - 300\left(\frac{C}{B}\right)^2 + 60\left(\frac{B}{C}\right) + 64\left(\frac{B}{C}\right)\left(\frac{PL}{B}\right) + 106\left(\frac{Ag}{B}\right)\left(\frac{PL}{B}\right) + 66\left(\frac{B}{Ag}\right) \quad (12)$$

$$\text{K28} = 309 - 388\left(\frac{C}{B}\right) - 154\left(\frac{C}{B}\right)\left(\frac{PL}{B}\right) + 168\left(\frac{C}{B}\right)^2 - 79\left(\frac{B}{C}\right) - 9.5\left(\frac{B}{Ag}\right) + 2595\left(\frac{PL}{B}\right)^2 \quad (13)$$

Finally, the third sub-model was concerned in predicting the environmental impact factor using six inputs cubic polynomials, which are (C/B, Ag/B, PL/B, Fc28, S and K28), hence, the polynomial has 84 possible terms (56+21+6+1=84) as follows:

$$\sum_{i=1}^{i=6}\sum_{j=1}^{j=6}\sum_{k=1}^{k=6} X_i.X_j.X_k + \sum_{i=1}^{i=6}\sum_{j=1}^{j=6} X_i.X_j + \sum_{i=1}^{i=6} X_i + C \quad (14)$$

GA technique was applied on these polynomials to select the most effective nine terms of each polynomial to predict P. The output is illustrated in Equation 15 and its fitness is shown in Figure 9. The error% and (R^2) values were (21.4% - 0.371).

$$\text{P} = -40.5 + 66\left(\frac{C}{B}\right) - 9.8\,\text{K28}\left(\frac{C}{B}\right) - 0.22\,\text{S}\left(\frac{C}{B}\right) - 4.3\left(\frac{Ag}{B}\right) + 0.53\,\text{K28}\left(\frac{Ag}{B}\right) + 2358\left(\frac{PL}{B}\right)^2 + 7.6\,\text{K28} + 0.21\,\text{S} \quad (15)$$

The results of all developed models are summarized in Table 7. Figure 9 compare the accuracies of the developed models graphically.

Table 7. Accuracies of developed models

Item	Technique	Model	SSE	Error %	R^2
Fc03	ANN	Figure 5, Table 4	1123	9.4	0.955
	EPR	Equation 2	1527	10.9	0.938
Fc07	ANN	Figure 5, Table 4	2093	8.5	0.947
	EPR	Equation 3	2837	9.9	0.926
Fc28	ANN	Figure 5, Table 4	2493	7.2	0.960
	EPR	Equation 4	4954	10.1	0.917
Fc60	ANN	Figure 5, Table 4	2740	6.9	0.965
	EPR	Equation 5	4817	9.2	0.936
Fc90	ANN	Figure 5, Table 4	3590	7.6	0.958
	EPR	Equation 6	5548	9.5	0.934
Ft28	ANN	Figure 5, Table 4	31	8.9	0.925
	EPR	Equation 7	33	9.2	0.920
Ff28	ANN	Figure 5, Table 4	81	8.7	0.944
	EPR	Equation 8	93	9.3	0.936
Fb28	ANN	Figure 5, Table 4	90	8.2	0.954
	EPR	Equation 9	131	9.9	0.931
S	ANN	Figure 6, Table 5	6026	7.6	0.878
	EPR	Equation 11	8068	8.7	0.831
Ec28	ANN	Figure 6, Table 5	516	5.9	0.949
	EPR	Equation 12	1088	8.6	0.887
K28	ANN	Figure 6, Table 5	11	7.4	0.946
	EPR	Equation 13	22	10.5	0.887
P	ANN	Figure 7, Table 6	26	6.8	0.960
	EPR	Equation 15	258	21.4	0.371

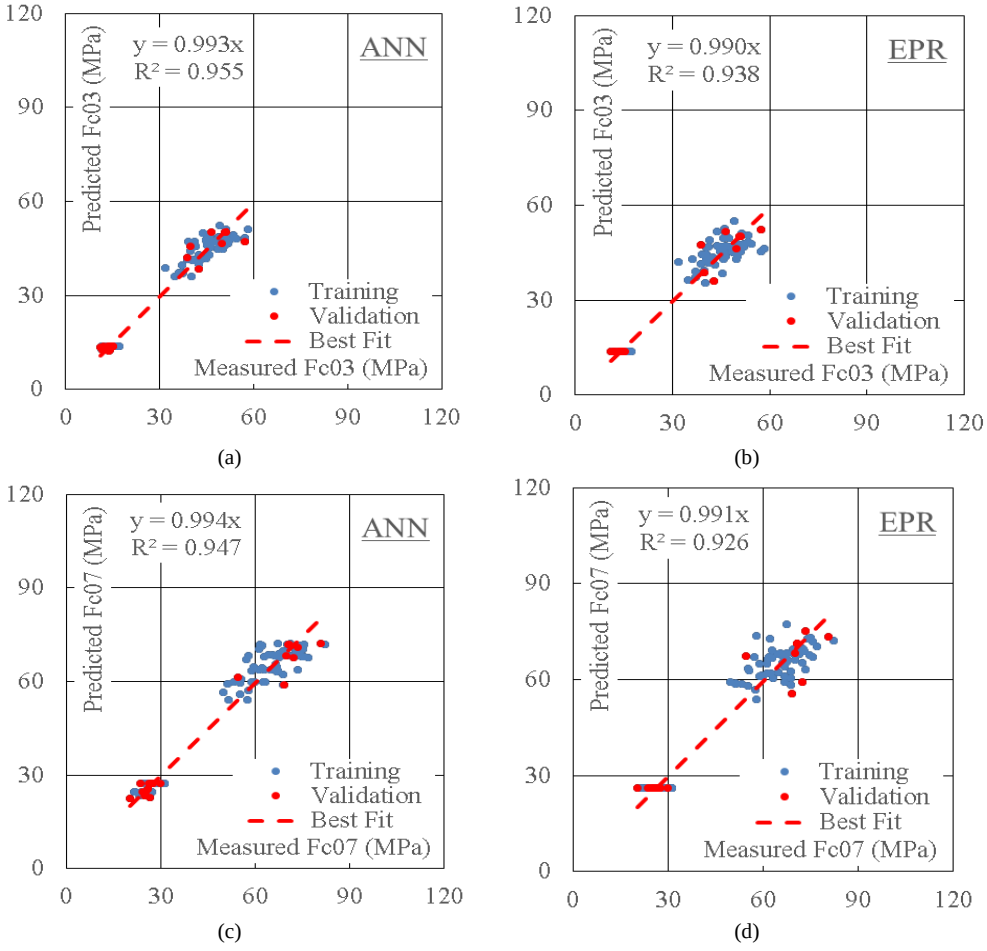

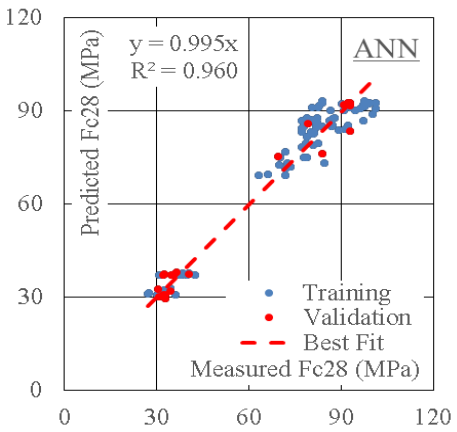
y = 0.995x
R² = 0.960
ANN
Predicted Fc28 (MPa)
Training
Validation
Best Fit
Measured Fc28 (MPa)
0
30
60
90
120

(e)

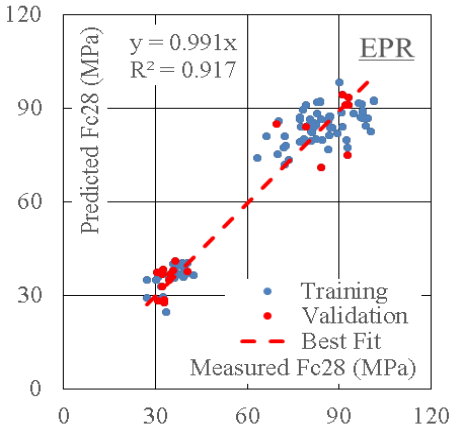
y = 0.991x
R² = 0.917
EPR
Predicted Fc28 (MPa)
Training
Validation
Best Fit
Measured Fc28 (MPa)
0
30
60
90
120

(f)

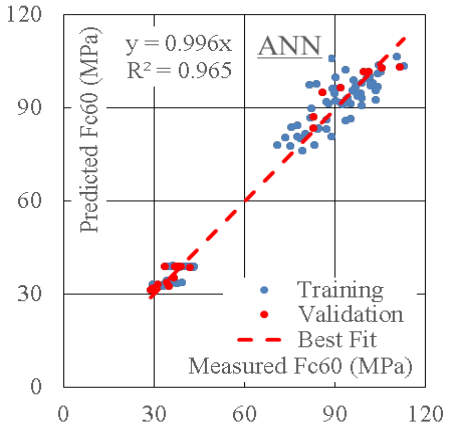
y = 0.996x
R² = 0.965
ANN
Predicted Fc60 (MPa)
Training
Validation
Best Fit
Measured Fc60 (MPa)
0
30
60
90
120

(g)

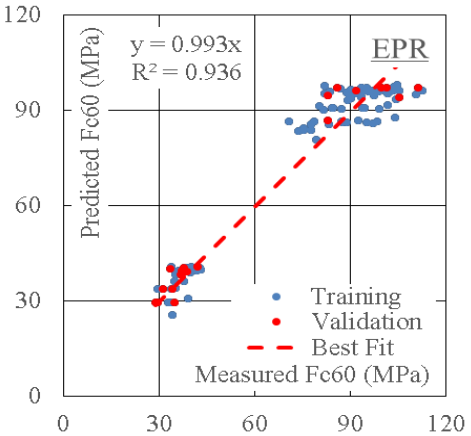
y = 0.993x
R² = 0.936
EPR
Predicted Fc60 (MPa)
Training
Validation
Best Fit
Measured Fc60 (MPa)
0
30
60
90
120

(h)

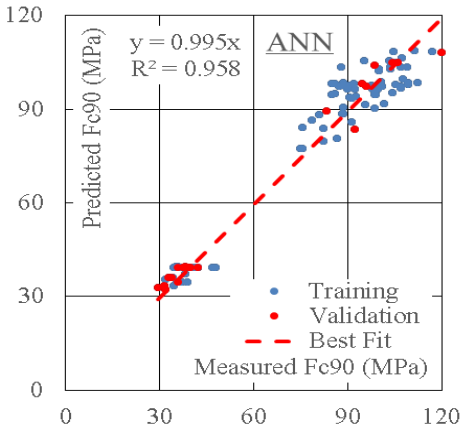
y = 0.995x
R² = 0.958
ANN
Predicted Fc90 (MPa)
Training
Validation
Best Fit
Measured Fc90 (MPa)
0
30
60
90
120

(i)

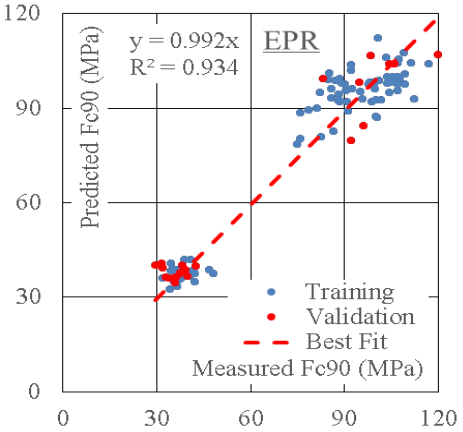
y = 0.992x
R² = 0.934
EPR
Predicted Fc90 (MPa)
Training
Validation
Best Fit
Measured Fc90 (MPa)
0
30
60
90
120

(j)

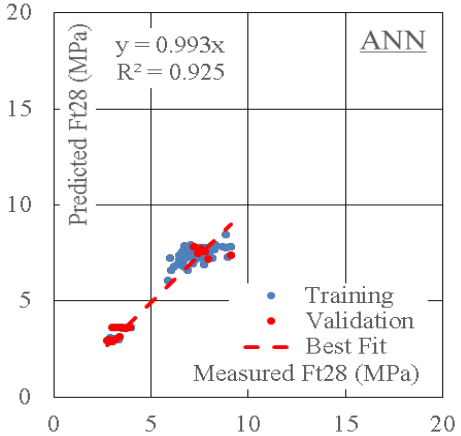
y = 0.993x
R² = 0.925
ANN
Predicted Ft28 (MPa)
Training
Validation
Best Fit
Measured Ft28 (MPa)
0
5
10
15
20

(k)

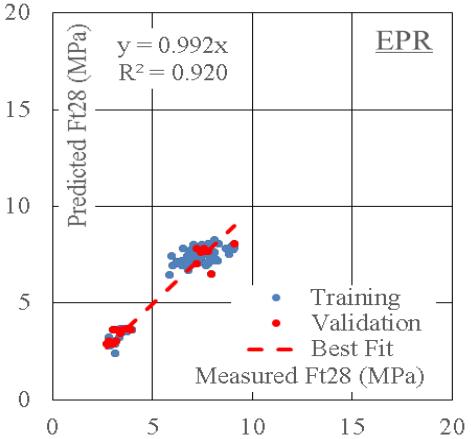
y = 0.992x
R² = 0.920
EPR
Predicted Ft28 (MPa)
Training
Validation
Best Fit
Measured Ft28 (MPa)
0
5
10
15
20

(l)

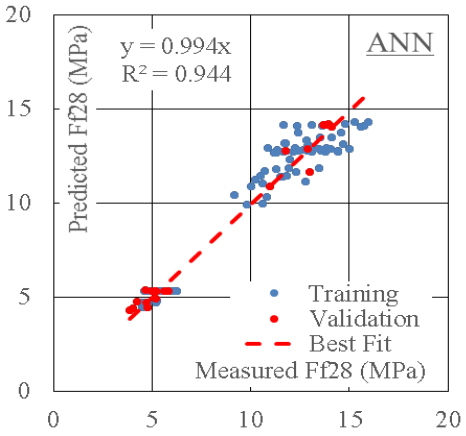
ANN
y = 0.994x
R² = 0.944
Predicted Ff28 (MPa)
Training
Validation
Best Fit
Measured Ff28 (MPa)

(m)

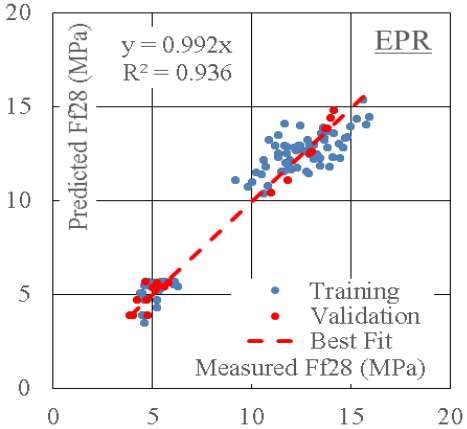
EPR
y = 0.992x
R² = 0.936
Predicted Ff28 (MPa)
Training
Validation
Best Fit
Measured Ff28 (MPa)

(n)

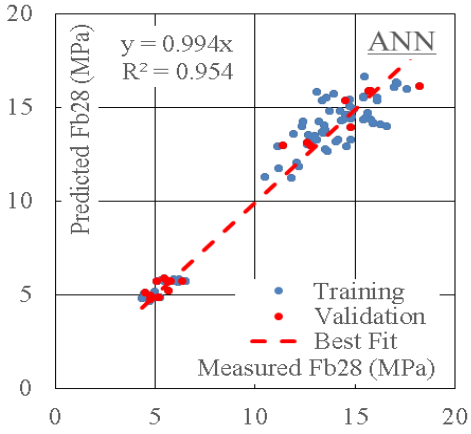
ANN
y = 0.994x
R² = 0.954
Predicted Fb28 (MPa)
Training
Validation
Best Fit
Measured Fb28 (MPa)

(o)

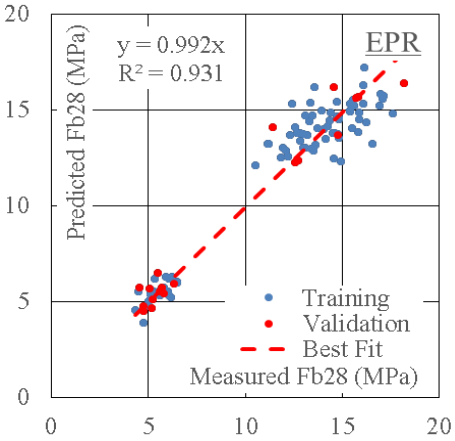
EPR
y = 0.992x
R² = 0.931
Predicted Fb28 (MPa)
Training
Validation
Best Fit
Measured Fb28 (MPa)

(p)

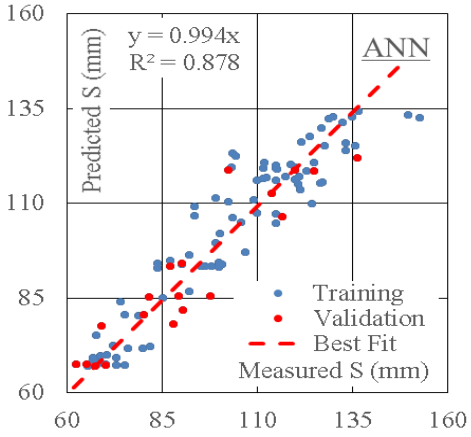
ANN
y = 0.994x
R² = 0.878
Predicted S (mm)
Training
Validation
Best Fit
Measured S (mm)

(q)

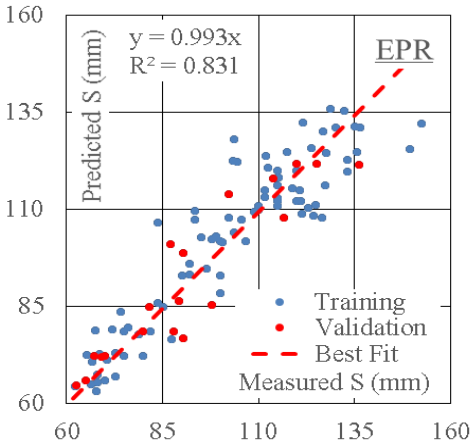
EPR
y = 0.993x
R² = 0.831
Predicted S (mm)
Training
Validation
Best Fit
Measured S (mm)

(r)

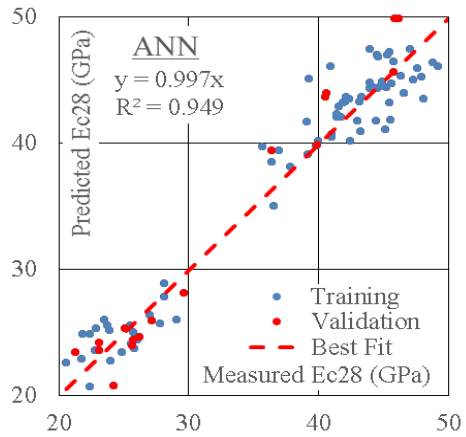
ANN
y = 0.997x
R² = 0.949
Predicted Ec28 (GPa)
Training
Validation
Best Fit
Measured Ec28 (GPa)

(s)

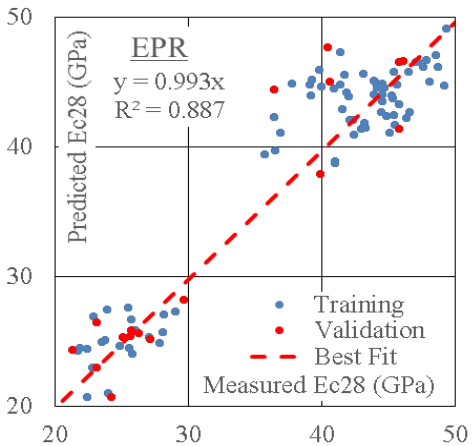
EPR
y = 0.993x
R² = 0.887
Predicted Ec28 (GPa)
Training
Validation
Best Fit
Measured Ec28 (GPa)

(t)

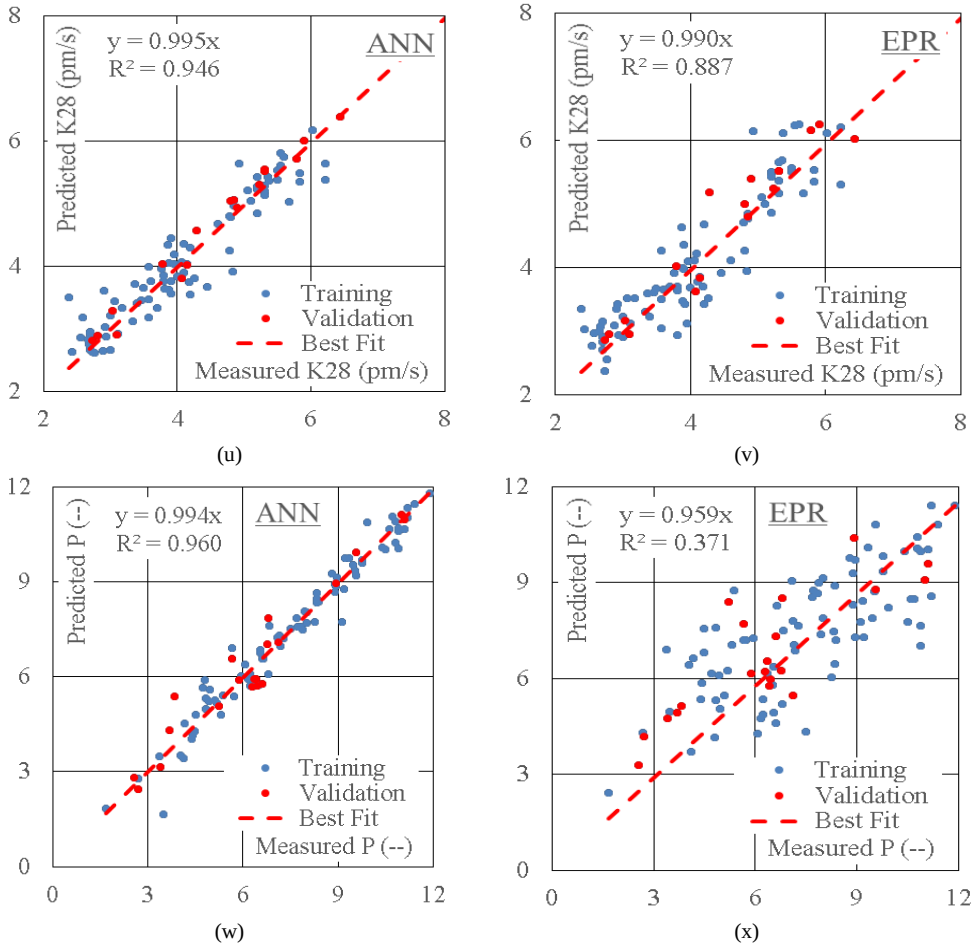

Figure 9. Relation between predicted and calculated values using the developed models

4.3. The Developed Mix Design Aid

Although the developed predicting models for (Fc28) using (ANN) and (EPR) are accurate enough, they are still hard to implement in practical mix designs, especially for manual calculations [91–96]. Hence, concrete mix design tools were developed by substituting in the developed ANN model different combinations of input parameter values that varied at constant intervals. Figure 10 presents the corresponding binder content (B) and water-binder ratio (W/B) for each input parameter combination, while the calculated (Fc28) values were plotted on the contour charts shown in Figure 11. The key chart indicates the changes in mix design when moving toward each side of the design chart; moving vertically changes the concrete strength and plasticizer-binder ratio, while moving horizontally changes the binder content and water-binder ratio.

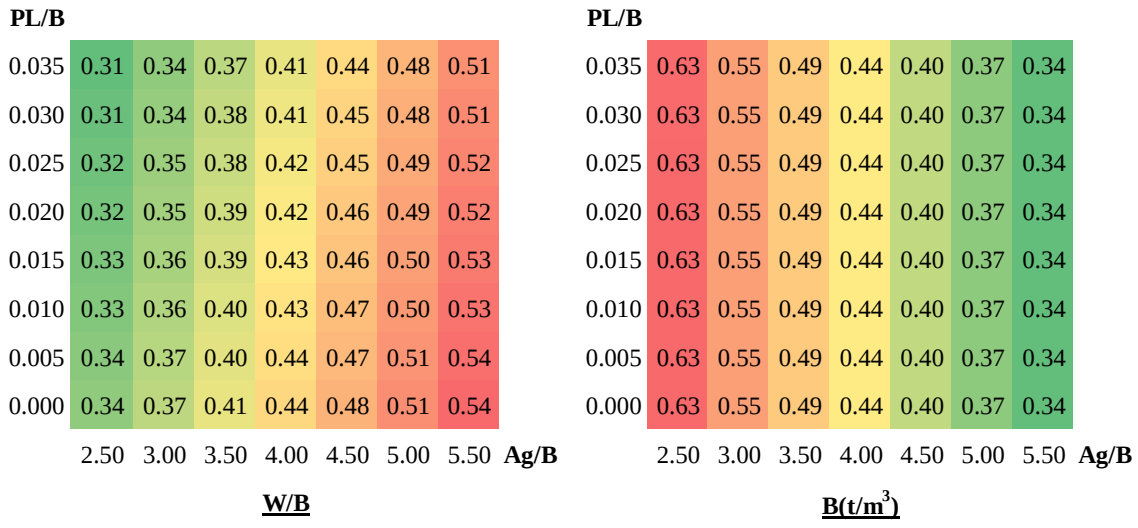

Figure 10. Concrete mix design aid, corresponding binder content (B) and water-binder ratio (W/B) for diffident combinations of (PL/B), (Ag/B)

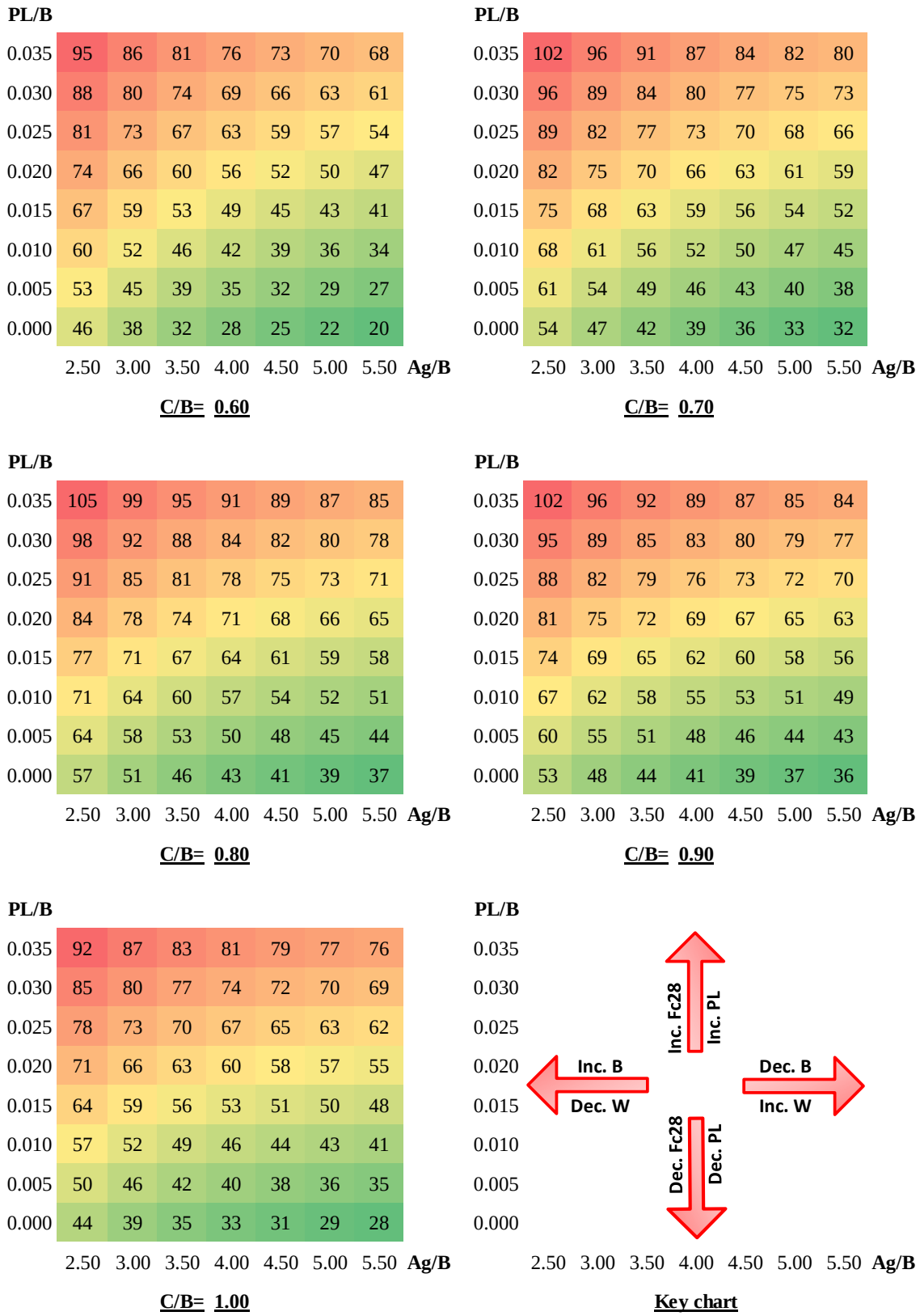

Figure 11. Concrete mix design aid, key chat, (Fc28) for diffident combinations of (PL/B), (Ag/B) & (C/B)

Using this tool is very simple, requiring only the desire (Fc28) and cement-binder ratio (C/B). Just select the correct chart in Figure 11 based on the (C/B) value, then locate the required (Fc28) on the selected chart to determine both (Ag/B) and (PL/B). From the corresponded cells in Figure 10, both binder content (B) (ton/m^3) and water-binder ratio (W/B) could be determined. Finally, the absolute values of water, plasticizer, cement, (fly ash or rich husk ash), and fine and coarse aggregates [92, 94] could be calculated by multiplying their ratios by the binder content, considering that the coarse aggregate content is twice the fine aggregate content.

For example, to design a concrete mix with (Fc28=60MPa) and (C/B=80%), the middle left chart in Figure 11 will be used, (Ag/B) is 3.5 and (PL/B) is 1%. From Figure 10, the binder content is 0.49 t/m^3 and (W/B) is 40%. Hence, 1.0 m3 of this mix contains 390kg cement, 100kg fly ash or rice husk ash, 195 litter of water, 4.9kg plasticizer, 570kg fine aggregate (sand) and 1140kg coarse aggregate.

5. Conclusions

This research presents three models using two techniques (ANN, and EPR) to predict concrete compressive strength at different ages (Fc03, Fc07, Fc28, Fc60, Fc90), splitting, flexural and bond strengths after 28 days (Ft28, Ff28 and Fb28), slump, elastic modulus and permeability after 28 days (S, Ec28 and K28) besides the environmental impact factor (P) using cement-binder ratio (C/B), total aggregate-binder ratio (Ag/B) and super-plasticizer-binder ratio (PL/B). Also, the research presented a concrete mix design tool developed based on the developed predictive models. The results of comparing the accuracies of the developed models could be concluded in the following points:

- Based on the correlations between the considered variables, the two developed models were constructed using three sub-models, the first to predict the strengths, the second to estimate the physical properties, and the third to evaluate the environmental impact factor.
- ANN models showed the best accuracy, with average values of 91.8%, 93.0%, and 93.2% for the three sub-models, respectively. The total average accuracy was 92.3%. In spate of its high accuracy, it is too difficult to implement manually. The developed mix design tool provides a quick and easy alternative to the long and complicated calculations of ANN.
- The EPR model presented a less complicated and also less accurate alternative for the ANN, where its accuracies were 90.3%, 90.7%, and 78.6% for the three sub-models, respectively. The total average accuracy was 89.4%.
- The limited accuracy of the third EPR sub-model indicated that the relation between P and the considered inputs is too complicated to be captured by polynomial regression, even for the optimized one. On the other hand, the highly complicated third ANN sub-model was capable of capturing this relationship accurately.
- The sum of the absolute weights of each neuron in the input layer of the developed third ANN sub-model indicated that P is almost equally affected by all input values, which is confirmed by the developed formula in the third EPR sub-model that contains all the considered inputs.
- The GA technique successfully reduced the 20, 35, and 84 terms of the conventional polynomial regression cubic formula to only 5, 7, and 9 terms for the three sub-models, respectively, without having a significant impact on its accuracy.
- Like any other regression technique, the generated formulas are valid within the considered range of parameter values; beyond this range, the prediction accuracy should be verified.
- Figures 10 and 11 present the mapping for (Fc28) values corresponding to all possible mix combinations (within the limits of the available dataset). Studying these charts leads to the following additional remarks.
- This tool (charts) is limited to the following ranges:
  - Binder content, 340 to 630 kg/m^3;
  - Water-binder ratio, 31% to 54%;
  - Fly ash or rice husk ash– binder ratio, 0.0% to 40%;
  - Total aggregate – binder ratio, 2.5 to 5.5;
  - Coarse –fine aggregate ratio is constant and equals to 2.0;
  - Fc28, 20 to 105 MPa.
- The maximum Fc28 values occur when the cement-binder ratio is 80%.
- Decreasing the aggregate-binder ratio increases the (Fc28) due to increased binder content and reduces the water-binder ratio, and vice versa.
- Increasing the plasticizer–binder ratio increases the concrete strength (Fc28) regardless of the cement-binder ratio.
- Further studies may be carried out to predict the same outputs using a wider range of databases that include high- and ultra-high-performance concrete, besides special types of concrete such as self-healing concrete.

6. Declarations

6.1. Author Contributions

Conceptualization, K.C.O.; methodology, A.M.E.; formal analysis, A.S.; investigation, H.J.; data curation, F.D.; writing—original draft preparation, K.C.O., A.M.E., A.S., H.J., F.D., and H.A.M.; writing—review and editing, K.C.O., A.M.E., A.S., H.J., F.D., and H.A.M.; supervision, H.A.M. All authors have read and agreed to the published version of the manuscript.

6.2. Data Availability Statement

The data presented in this study are available in the article.

6.3. Funding

The authors received no financial support for the research, authorship, and/or publication of this article.

6.4. Conflicts of Interest

The authors declare no conflict of interest.

7. References

[1] Kamiya, K., Oka, A., Nasu, H., & Hashimoto, T. (2000). Comparative study of structure of silica gels from different sources. Journal of Sol-Gel Science and Technology, 19(1–3), 495–499. doi:10.1023/A:1008720118475.

[2] Maraghechi, H., Avet, F., Wong, H., Kamyab, H., & Scrivener, K. (2018). Performance of Limestone Calcined Clay Cement (LC3) with various kaolinite contents with respect to chloride transport. Materials and Structures/Materiaux et Constructions, 51(5), 125. doi:10.1617/s11527-018-1255-3.

[3] Pillai, R. G., Gettu, R., Santhanam, M., Rengaraju, S., Dhandapani, Y., Rathnarajan, S., & Basavaraj, A. S. (2019). Service life and life cycle assessment of reinforced concrete systems with limestone calcined clay cement (LC3). Cement and Concrete Research, 118, 111–119. doi:10.1016/j.cemconres.2018.11.019.

[4] Danner, T., Norden, G., & Justnes, H. (2018). Characterisation of calcined raw clays suitable as supplementary cementitious materials. Applied Clay Science, 162, 391–402. doi:10.1016/j.clay.2018.06.030.

[5] Yang, X., Teng, F., & Wang, G. (2013). Incorporating environmental co-benefits into climate policies: A regional study of the cement industry in China. Applied Energy, 112, 1446–1453. doi:10.1016/j.apenergy.2013.03.040.

[6] Li, C., Nie, Z., Cui, S., Gong, X., Wang, Z., & Meng, X. (2014). The life cycle inventory study of cement manufacture in China. Journal of Cleaner Production, 72, 204–211. doi:10.1016/j.jclepro.2014.02.048.

[7] Oh, D. Y., Noguchi, T., Kitagaki, R., & Park, W. J. (2014). CO2 emission reduction by reuse of building material waste in the Japanese cement industry. Renewable and Sustainable Energy Reviews, 38, 796–810. doi:10.1016/j.rser.2014.07.036.

[8] Saeli, M., Novais, R. M., Seabra, M. P., & Labrincha, J. A. (2018). Green geopolymeric concrete using grits for applications in construction. Materials Letters, 233, 94–97. doi:10.1016/j.matlet.2018.08.102.

[9] Thomas, B. S., & Chandra Gupta, R. (2016). Properties of high strength concrete containing scrap tire rubber. Journal of Cleaner Production, 113, 86–92. doi:10.1016/j.jclepro.2015.11.019.

[10] Thomas, B. S., & Gupta, R. C. (2015). Long term behaviour of cement concrete containing discarded tire rubber. Journal of Cleaner Production, 102, 78–87. doi:10.1016/j.jclepro.2015.04.072.

[11] Siddique, R., Singh, K., Kunal, P., Singh, M., Corinaldesi, V., & Rajor, A. (2016). Properties of bacterial rice husk ash concrete. Construction and Building Materials, 121, 112–119. doi:10.1016/j.conbuildmat.2016.05.146.

[12] Kumar, S., Gupta, R. C., Shrivastava, S., Csetenyi, L., & Thomas, B. S. (2016). Preliminary study on the use of quartz sandstone as a partial replacement of coarse aggregate in concrete based on clay content, morphology and compressive strength of combined gradation. Construction and Building Materials, 107, 103–108. doi:10.1016/j.conbuildmat.2016.01.004.

[13] Mehra, P., Gupta, R. C., & Thomas, B. S. (2016). Properties of concrete containing jarosite as a partial substitute for fine aggregate. Journal of Cleaner Production, 120, 241–248. doi:10.1016/j.jclepro.2016.01.015.

[14] Mehra, P., Gupta, R. C., & Thomas, B. S. (2016). Assessment of durability characteristics of cement concrete containing jarosite. Journal of Cleaner Production, 119, 59–65. doi:10.1016/j.jclepro.2016.01.055.

[15] Thomas, B. S., Damare, A., & Gupta, R. C. (2013). Strength and durability characteristics of copper tailing concrete. Construction and Building Materials, 48, 894–900. doi:10.1016/j.conbuildmat.2013.07.075.

[16] Thomas, B. S., Gupta, R. C., & Panicker, V. J. (2016). Recycling of waste tire rubber as aggregate in concrete: Durability-related performance. Journal of Cleaner Production, 112, 504–513. doi:10.1016/j.jclepro.2015.08.046.

[17] Pradhan, S., Chang Boon Poh, A., & Qian, S. (2022). Impact of service life and system boundaries on life cycle assessment of sustainable concrete mixes. Journal of Cleaner Production, 342, 130847. doi:10.1016/j.jclepro.2022.130847.

[18] Valipour, M., Shekarchi, M., & Arezoumandi, M. (2017). Chlorine diffusion resistivity of sustainable green concrete in harsh marine environments. Journal of Cleaner Production, 142, 4092–4100. doi:10.1016/j.jclepro.2016.10.015.

[19] Al-Khalaf, M. N., & Yousif, H. A. (1984). Use of rice husk ash in concrete. International Journal of Cement Composites and Lightweight Concrete, 6(4), 241–248. doi:10.1016/0262-5075(84)90019-8.

[20] James, J., & Subba Rao, M. (1986). Reactivity of rice husk ash. Cement and Concrete Research, 16(3), 296–302. doi:10.1016/0008-8846(86)90104-3.

[21] Saraswathy, V., & Song, H. W. (2007). Corrosion performance of rice husk ash blended concrete. Construction and Building Materials, 21(8), 1779–1784. doi:10.1016/j.conbuildmat.2006.05.037.

[22] Thomas, B. S., Gupta, R. C., Mehra, P., & Kumar, S. (2015). Performance of high strength rubberized concrete in aggressive environment. Construction and Building Materials, 83, 320–326. doi:10.1016/j.conbuildmat.2015.03.012.

[23] Thomas, B. S., Gupta, R. C., & John Panicker, V. (2015). Experimental and modelling studies on high strength concrete containing waste tire rubber. Sustainable Cities and Society, 19, 68–73. doi:10.1016/j.scs.2015.07.013.

[24] Valipour, M., Pargar, F., Shekarchi, M., & Khani, S. (2013). Comparing a natural pozzolan, zeolite, to metakaolin and silica fume in terms of their effect on the durability characteristics of concrete: A laboratory study. Construction and Building Materials, 41, 879–888. doi:10.1016/j.conbuildmat.2012.11.054.

[25] Wang, Y., Tan, Y., Wang, Y., & Liu, C. (2020). Mechanical properties and chloride permeability of green concrete mixed with fly ash and coal gangue. Construction and Building Materials, 233, 117166. doi:10.1016/j.conbuildmat.2019.117166.

[26] Tkaczewska, E. (2014). Effect of the superplasticizer type on the properties of the fly ash blended cement. Construction and Building Materials, 70, 388–393. doi:10.1016/j.conbuildmat.2014.07.096.

[27] Shehab, H. K., Eisa, A. S., & Wahba, A. M. (2016). Mechanical properties of fly ash based geopolymer concrete with full and partial cement replacement. Construction and Building Materials, 126, 560–565. doi:10.1016/j.conbuildmat.2016.09.059.

[28] Khodair, Y., & Raza, M. (2017). Sustainable self-consolidating concrete using recycled asphalt pavement and high volume of supplementary cementitious materials. Construction and Building Materials, 131, 245–253. doi:10.1016/j.conbuildmat.2016.11.044.

[29] Givi, A. N., Rashid, S. A., Aziz, F. N. A., & Salleh, M. A. M. (2010). Assessment of the effects of rice husk ash particle size on strength, water permeability and workability of binary blended concrete. Construction and Building Materials, 24(11), 2145–2150. doi:10.1016/j.conbuildmat.2010.04.045.

[30] Gursel, A. P., Maryman, H., & Ostertag, C. (2016). A life-cycle approach to environmental, mechanical, and durability properties of "green" concrete mixes with rice husk ash. Journal of Cleaner Production, 112, 823–836. doi:10.1016/j.jclepro.2015.06.029.

[31] Mazlum, F., & Uyan, M. (1992). Strength of Mortar Made with Cement Containing Rice Husk Ash and Cured in Sodium Sulfate Solution. Special Publication, 132, 513-532.

[32] Mehta, P. K. (1986). Concrete. Structure, properties and materials. Prentice Hall, Hoboken, United States.

[33] Zhang, M. H., & Malhotra, V. M. (1996). High-performance concrete incorporating rice husk ash as a supplementary cementing material. ACI Materials Journal, 93(6), 629–636. doi:10.14359/9870.

[34] McLellan, B. C., Williams, R. P., Lay, J., Van Riessen, A., & Corder, G. D. (2011). Costs and carbon emissions for geopolymer pastes in comparison to ordinary Portland cement. Journal of Cleaner Production, 19(9–10), 1080–1090. doi:10.1016/j.jclepro.2011.02.010.

[35] Amin, M., & Abdelsalam, B. A. (2019). Efficiency of rice husk ash and fly ash as reactivity materials in sustainable concrete. Sustainable Environment Research, 29(1), 1-10. doi:10.1186/s42834-019-0035-2.

[36] Mater, Y., Kamel, M., Karam, A., & Bakhoum, E. (2022). ANN-Python prediction model for the compressive strength of green concrete. Construction Innovation. doi:10.1108/CI-08-2021-0145.

[37] Naseri, H., Jahanbakhsh, H., Khezri, K., & Shirzadi Javid, A. A. (2022). Toward sustainability in optimizing the fly ash concrete mixture ingredients by introducing a new prediction algorithm. Environment, Development and Sustainability, 24(2), 2767–2803. doi:10.1007/s10668-021-01554-2.

[38] Bheel, N., keerio, M. A., Kumar, A., Shahzaib, J., Ali, Z., Ali, M., & sohu, S. (2022). An Investigation on Fresh and Hardened Properties of Concrete Blended with Rice Husk Ash as Cementitious Ingredient and Coal Bottom Ash as Sand Replacement Material. Silicon, 14(2), 677–688. doi:10.1007/s12633-020-00906-3.

[39] Patnaik, B., Buony, G., Mekuria, Z. (2022). Rice Husk Ash as a Sustainable Cementing Material for Concrete in Ethiopia. Recent Developments in Sustainable Infrastructure (ICRDSI-2020)—Structure and Construction Management. Lecture Notes in Civil Engineering, 21. Springer, Singapore. doi:10.1007/978-981-16-8433-3_43.

[40] Gursel, A. P. (2014). Life-cycle assessment of concrete: decision-support tool and case study application. PhD Thesis, University of California, Berkeley, United States.

[41] Pradhan, S., Tiwari, B. R., Kumar, S., & Barai, S. V. (2019). Comparative LCA of recycled and natural aggregate concrete using Particle Packing Method and conventional method of design mix. Journal of Cleaner Production, 228, 679–691. doi:10.1016/j.jclepro.2019.04.328.

[42] Ehrlich, B. (2010). Reducing environmental impacts of cement and concrete. Environmental Building News, BuildingGreen, Inc. Available online: https://www.buildinggreen.com/feature/reducing-environmental-impacts-cement-and-concrete (accessed on May 2022).

[43] Dabbaghi, F., Sadeghi-Nik, A., Ali Libre, N., & Nasrollahpour, S. (2021). Characterizing fiber reinforced concrete incorporating zeolite and metakaolin as natural pozzolans. Structures, 34, 2617–2627. doi:10.1016/j.istruc.2021.09.025.

[44] Mousavi, M. A., Sadeghi-Nik, A., Bahari, A., Jin, C., Ahmed, R., Ozbakkaloglu, T., & de Brito, J. (2021). Strength optimization of cementitious composites reinforced by carbon nanotubes and Titania nanoparticles. Construction and Building Materials, 303(124510). doi:10.1016/j.conbuildmat.2021.124510.

[45] Bahari, A., Sadeghi-Nik, A., Shaikh, F. U. A., Sadeghi-Nik, A., Cerro-Prada, E., Mirshafiei, E., & Roodbari, M. (2022). Experimental studies on rheological, mechanical, and microstructure properties of self-compacting concrete containing perovskite nanomaterial. Structural Concrete, 23(1), 564-578. doi:10.1002/suco.202000548.

[46] Kafi, M. A., Sadeghi-Nik, A., Bahari, A., Sadeghi-Nik, A., & Mirshafiei, E. (2016). Microstructural Characterization and Mechanical Properties of Cementitious Mortar Containing Montmorillonite Nanoparticles. Journal of Materials in Civil Engineering, 28(12). doi:10.1061/(asce)mt.1943-5533.0001671.

[47] Li, Y., Han, D., Wang, H., Lyu, H., & Zou, D. (2022). Carbonation curing of mortars produced with reactivated cementitious materials for CO2 sequestration. Journal of Cleaner Production, 135501. doi: 10.1016/j.jclepro.2022.135501.

[48] Amiri, H., Azadi, S., Karimaei, M., Sadeghi, H., & Farshad Dabbaghi. (2022). Multi-objective optimization of coal waste recycling in concrete using response surface methodology. Journal of Building Engineering, 45(103472). doi:10.1016/j.jobe.2021.103472.

[49] Rashad, A. M. (2018). Lightweight expanded clay aggregate as a building material – An overview. Construction and Building Materials, 170, 757–775. doi:10.1016/j.conbuildmat.2018.03.009.

[50] Bahari, A., Berenjian, J., & Sadeghi-Nik, A. (2016). Modification of Portland cement with Nano SiC. Proceedings of the National Academy of Sciences, India Section A: Physical Sciences, 86(3), 323–331. doi:10.1007/s40010-015-0244-y.

[51] Sadeghi-Nik, A., Berenjian, J., Alimohammadi, S., Lotfi-Omran, O., Sadeghi-Nik, A., & Karimaei, M. (2019). The Effect of Recycled Concrete Aggregates and Metakaolin on the Mechanical Properties of Self-Compacting Concrete Containing Nanoparticles. Iranian Journal of Science and Technology - Transactions of Civil Engineering, 43, 503–515. doi:10.1007/s40996-018-0182-4.

[52] Dabbaghi, F., Tanhadoust, A., Nehdi, M. L., Nasrollahpour, S., Dehestani, M., & Yousefpour, H. (2021). Life cycle assessment multi-objective optimization and deep belief network model for sustainable lightweight aggregate concrete. Journal of Cleaner Production, 318(128554). doi:10.1016/j.jclepro.2021.128554.

[53] Sadeghi-Nik, A., Berenjian, J., Bahari, A., Safaei, A. S., & Dehestani, M. (2017). Modification of microstructure and mechanical properties of cement by nanoparticles through a sustainable development approach. Construction and Building Materials, 155, 880–891. doi:10.1016/j.conbuildmat.2017.08.107.

[54] Bahari, A., Sadeghi-Nik, A., Roodbari, M., Sadeghi-Nik, A., & Mirshafiei, E. (2018). Experimental and theoretical studies of ordinary Portland cement composites contains nano LSCO perovskite with Fokker-Planck and chemical reaction equations. Construction and Building Materials, 163, 247–255. doi:10.1016/j.conbuildmat.2017.12.073.

[55] Dabbaghi, F., Nasrollahpour, S., Dehestani, M., & Yousefpour, H. (2022). Optimization of Concrete Mixtures Containing Lightweight Expanded Clay Aggregates Based on Mechanical, Economical, Fire-Resistance, and Environmental Considerations. Journal of Materials in Civil Engineering, 34(2). doi:10.1061/(asce)mt.1943-5533.0004083.

[56] Bajpai, R., Choudhary, K., Srivastava, A., Sangwan, K. S., & Singh, M. (2020). Environmental impact assessment of fly ash and silica fume based geopolymer concrete. Journal of Cleaner Production, 254(120147). doi:10.1016/j.jclepro.2020.120147.

[57] Habert, G., D'Espinose De Lacaillerie, J. B., & Roussel, N. (2011). An environmental evaluation of geopolymer based concrete production: Reviewing current research trends. Journal of Cleaner Production, 19(11), 1229–1238. doi:10.1016/j.jclepro.2011.03.012.

[58] Dabbaghi, F., Fallahnejad, H., Nasrollahpour, S., Dehestani, M., & Yousefpour, H. (2021). Evaluation of fracture energy, toughness, brittleness, and fracture process zone properties for lightweight concrete exposed to high temperatures. Theoretical and Applied Fracture Mechanics, 116(103088). doi:10.1016/j.tafmec.2021.103088.

[59] Zhang, Y., Luo, W., Wang, J., Wang, Y., Xu, Y., & Xiao, J. (2019). A review of life cycle assessment of recycled aggregate concrete. Construction and Building Materials, 209, 115–125. doi:10.1016/j.conbuildmat.2019.03.078.

[60] Juenger, M. C. G., & Siddique, R. (2015). Recent advances in understanding the role of supplementary cementitious materials in concrete. Cement and Concrete Research, 78, 71–80. doi:10.1016/j.cemconres.2015.03.018.

[61] Rashidi, M., Joshaghani, A., & Ghodrat, M. (2020). Towards eco-flowable concrete production. Sustainability (Switzerland), 12(3), 1–17. doi:10.3390/su12031208.

[62] Dabbaghi, F., Dehestani, M., Yousefpour, H., Rasekh, H., & Navaratnam, S. (2021). Residual compressive stress–strain relationship of lightweight aggregate concrete after exposure to elevated temperatures. Construction and Building Materials, 298(123890). doi:10.1016/j.conbuildmat.2021.123890.

[63] Amin, M. N., Iqtidar, A., Khan, K., Javed, M. F., Shalabi, F. I., & Qadir, M. G. (2021). Comparison of machine learning approaches with traditional methods for predicting the compressive strength of rice husk ash concrete. Crystals, 11(7). doi:10.3390/cryst11070779.

[64] Bui, D. D., Hu, J., & Stroeven, P. (2005). Particle size effect on the strength of rice husk ash blended gap-graded Portland cement concrete. Cement and Concrete Composites, 27(3), 357–366. doi:10.1016/j.cemconcomp.2004.05.002.

[65] Fan, K., Li, D., Damrongwiriyanupap, N., & Li, L. yuan. (2019). Compressive stress-strain relationship for fly ash concrete under thermal steady state. Cement and Concrete Composites, 104(103371). doi:10.1016/j.cemconcomp.2019.103371.

[66] Naik, T. R. (2008). Sustainability of Concrete Construction. Practice Periodical on Structural Design and Construction, 13(2), 98–103. doi:10.1061/(asce)1084-0680(2008)13:2(98).

[67] Mathew, G., & Joseph, B. (2018). Flexural behaviour of geopolymer concrete beams exposed to elevated temperatures. Journal of Building Engineering, 15, 311–317. doi:10.1016/j.jobe.2017.09.009.

[68] Adamu, M., Trabanpruek, P., Jongvivatsakul, P., Likitlersuang, S., & Iwanami, M. (2021). Mechanical performance and optimization of high-volume fly ash concrete containing plastic wastes and graphene nanoplatelets using response surface methodology. Construction and Building Materials, 308(125085). doi:10.1016/j.conbuildmat.2021.125085.

[69] Shaikh, F. U. A., & Supit, S. W. M. (2015). Compressive strength and durability properties of high volume fly ash (HVFA) concretes containing ultrafine fly ash (UFFA). Construction and Building Materials, 82, 192–205. doi:10.1016/j.conbuildmat.2015.02.068.

[70] Siddique, R. (2004). Performance characteristics of high-volume Class F fly ash concrete. Cement and Concrete Research, 34(3), 487–493. doi:10.1016/j.cemconres.2003.09.002.

[71] Gartner, E. (2004). Industrially interesting approaches to "low-CO2" cements. Cement and Concrete Research, 34(9), 1489–1498. doi:10.1016/j.cemconres.2004.01.021.

[72] Thomas, B. S. (2018). Green concrete partially comprised of rice husk ash as a supplementary cementitious material – A comprehensive review. Renewable and Sustainable Energy Reviews, 82, 3913–3923. doi:10.1016/j.rser.2017.10.081.

[73] Dabbaghi, F., Dehestani, M., & Yousefpour, H. (2022). Residual mechanical properties of concrete containing lightweight expanded clay aggregate (LECA) after exposure to elevated temperatures. Structural Concrete, 23(4), 2162–2184. doi:10.1002/suco.202000821.

[74] Khan, K., Ullah, M. F., Shahzada, K., Amin, M. N., Bibi, T., Wahab, N., & Aljaafari, A. (2020). Effective use of micro-silica extracted from rice husk ash for the production of high-performance and sustainable cement mortar. Construction and Building Materials, 258(119589). doi:10.1016/j.conbuildmat.2020.119589.

[75] Ebid, A. M., Deifalla, A. F., & Mahdi, H. A. (2022). Evaluating Shear Strength of Light-Weight and Normal-Weight Concretes through Artificial Intelligence. Sustainability, 14(21), 14010. doi:10.3390/su142114010.

[76] Penadés-Plà, V., Martí, J. V., García-Segura, T., & Yepes, V. (2017). Life-cycle assessment: A comparison between two optimal post-tensioned concrete box-girder road bridges. Sustainability (Switzerland), 9(10). doi:10.3390/su9101864.

[77] O'Brien, K. R., Ménaché, J., & O'Moore, L. M. (2009). Impact of fly ash content and fly ash transportation distance on embodied greenhouse gas emissions and water consumption in concrete. International Journal of Life Cycle Assessment, 14(7), 621–629. doi:10.1007/s11367-009-0105-5.

[78] AzariJafari, H., Taheri Amiri, M. J., Ashrafian, A., Rasekh, H., Barforooshi, M. J., & Berenjian, J. (2019). Ternary blended cement: An eco-friendly alternative to improve resistivity of high-performance self-consolidating concrete against elevated temperature. Journal of Cleaner Production, 223, 575–586. doi:10.1016/j.jclepro.2019.03.054.

[79] Seto, K. E., Churchill, C. J., & Panesar, D. K. (2017). Influence of fly ash allocation approaches on the life cycle assessment of cement-based materials. Journal of Cleaner Production, 157, 65–75. doi:10.1016/j.jclepro.2017.04.093.

[80] Celik, K., Meral, C., Petek Gursel, A., Mehta, P. K., Horvath, A., & Monteiro, P. J. M. (2015). Mechanical properties, durability, and life-cycle assessment of self-consolidating concrete mixtures made with blended portland cements containing fly ash and limestone powder. Cement and Concrete Composites, 56, 59–72. doi:10.1016/j.cemconcomp.2014.11.003.

[81] Pitroda, J., Zala, L. B., & Umrigar, F. S. (2012). Experimental Investigations on Partial Replacement of Cement with Fly ash in design mix concrete. International Journal of Advanced Engineering Technology, 3(4), 126-129.

[82] Saha, A. K. (2018). Effect of class F fly ash on the durability properties of concrete. Sustainable Environment Research, 28(1), 25–31. doi:10.1016/j.serj.2017.09.001.

[83] Giaccio, G. M., & Malhotra, V. M. (1988). Concrete incorporating high volumes of ASTM Class F fly ash. Cement, Concrete and Aggregates, 10(2), 88–95. doi:10.1520/cca10088j.

[84] Feldman, R. F., Carette, G. G., & Malhotra, V. M. (1990). Studies on mechanics of development of physical and mechanical properties of high-volume fly ash-cement pastes. Cement and Concrete Composites, 12(4), 245–251. doi:10.1016/0958-9465(90)90003-G.

[85] Bouzoubaâ, N., Zhang, M. H., & Malhotra, V. M. (2001). Mechanical properties and durability of concrete made with high-volume fly ash blended cements using a coarse fly ash. Cement and Concrete Research, 31(10), 1393–1402. doi:10.1016/S0008-8846(01)00592-0.

[86] Poon, C. S., Lam, L., & Wong, Y. L. (2000). Study on high strength concrete prepared with large volumes of low calcium fly ash. Cement and Concrete Research, 30(3), 447–455. doi:10.1016/S0008-8846(99)00271-9.

[87] Ameri, F., Shoaei, P., Bahrami, N., Vaezi, M., & Ozbakkaloglu, T. (2019). Optimum rice husk ash content and bacterial concentration in self-compacting concrete. Construction and Building Materials, 222, 796–813. doi:10.1016/j.conbuildmat.2019.06.190.

[88] Iqtidar, A., Khan, N. B., Kashif-ur-Rehman, S., Javed, M. F., Aslam, F., Alyousef, R., Alabduljabbar, H., & Mosavi, A. (2021). Prediction of compressive strength of rice husk ash concrete through different machine learning processes. Crystals, 11(4). doi:10.3390/cryst11040352.

[89] Iftikhar, B., Alih, S. C., Vafaei, M., Elkotb, M. A., Shutaywi, M., Javed, M. F., Deebani, W., Khan, M. I., & Aslam, F. (2022). Predictive modeling of compressive strength of sustainable rice husk ash concrete: Ensemble learner optimization and comparison. Journal of Cleaner Production, 348(131285). doi:10.1016/j.jclepro.2022.131285.

[90] Onyelowe, K. C., Ebid, A. M., Mahdi, H. A., Riofrio, A., Eidgahee, D. R., Baykara, H., Soleymani, A., Kontoni, D.-P. N., Shakeri, J., & Jahangir, H. (2022). Optimal Compressive Strength of RHA Ultra-High-Performance Lightweight Concrete (UHPLC) and Its Environmental Performance Using Life Cycle Assessment. Civil Engineering Journal, 8(11), 2391–2410. doi:10.28991/cej-2022-08-11-03.

[91] Onyelowe, K. C., Ebid, A. M., Riofrio, A., Soleymani, A., Baykara, H., Kontoni, D. P. N., Mahdi, H. A., & Jahangir, H. (2022). Global warming potential-based life cycle assessment and optimization of the compressive strength of fly ash-silica fume concrete; environmental impact consideration. Frontiers in Built Environment, 8(992552). doi:10.3389/fbuil.2022.992552.

[92] Dao, P.-L., Bui, V.-D., Onyelowe, K. C., Ebid, A. M., Le, V. D., & Ahaneku, I. E. (2022). Effect of metakaolin on the mechanical properties of lateritic soil. Geotechnical Research, 9(4), 211–218. doi:10.1680/jgere.22.00046.

[93] Onyelowe, K. C., Ebid, A. M., Mahdi, H. A., Soleymani, A., Jayabalan, J., Jahangir, H., Samui, P., & Singh, R. P. (2022). Modeling the confined compressive strength of CFRP-jacketed noncircular concrete columns using artificial intelligence techniques. Cogent Engineering, 9(1). doi:10.1080/23311916.2022.2122156.

[94] Onyelowe, K. C., Gnananandarao, T., Ebid, A. M., Mahdi, H. A., Razzaghian Ghadikolaee, M., & Al-Ajamee, M. (2022). Evaluating the Compressive Strength of Recycled Aggregate Concrete Using Novel Artificial Neural Network. Civil Engineering Journal (Iran), 8(8), 1679–1693. doi:10.28991/CEJ-2022-08-08-011.

[95] Onyelowe, K. C., Ebid, A. M., Riofrio, A., Baykara, H., Soleymani, A., Mahdi, H. A., Jahangir, H., & Ibe, K. (2022). Multi-Objective Prediction of the Mechanical Properties and Environmental Impact Appraisals of Self-Healing Concrete for Sustainable Structures. Sustainability (Switzerland), 14(15). doi:10.3390/su14159573.

[96] Onyelowe, K. C., Kontoni, D. P. N., Ebid, A. M., Dabbaghi, F., Soleymani, A., Jahangir, H., & Nehdi, M. L. (2022). Multi-Objective Optimization of Sustainable Concrete Containing Fly Ash Based on Environmental and Mechanical Considerations. Buildings, 12(7), 948. doi:10.3390/buildings12070948.